Table 3. Derived pharmacokinetic parameters of lapatinib (including 95% confidence intervals)

Dose (mg/day)[a]	Geometric mean C_{max} (ng/ml)		Mean CSS_{max} (ng/ml)	Median t_{max} (h)		Geometric mean AUC (h ng/ml)[b]		Median $t_{1/2}$ (h)	
	Day 1	Day 21	Day 21	Day 1	Day 21	Day 1	Day 21	Day 1	Day 21
900	1011 (694–1472)	1895 (1319–2721)	857 (386–1234)	4.0 (2.0–6.0)	4.0 (3.0–6.0)	17 577 (11 812–26 154)	29 272 (21 618–39 638)	12.9 (10.1–18.3)	23.1 (9.8–38.2)
1200	1027 (474–2227)	1715 (965–3048)	820 (226–1308)	3.5 (2.1–6.0)	3.6 (3.0–7.9)	15 441 (7410–32 176)	25 680 (13 728–48 038)	11.5 (10.1–19.5)	16.9 (15.1–34.3)
1600	1538 (1042–2268)	3111 (1937–4996)	1899 (818–4357)	4.0 (2.0–8.0)	5.1 (0.9–8.0)	26 361 (17 519–39 665)	51 099 (28 674–91 062)	13.9 (9.6–18.0)	26.2 (12.9–48.3)
1800	1227 (465–3242)	2333 (927–5870)	1528 (586–3393)	3.9 (3.0–8.0)	3.9 (3.0–7.3)	32 841 (18 884–57 114)	39 451 (14 909–104 391)	15.7 (11.0–133.1)	21.8 (18.5–104.5)

AUC, area under the plasma drug concentration–time curve; C_{max}, maximum serum concentration; CSS_{max}, mean steady state maximum serum concentration; t_{max}, time to reach C_{max}; $t_{1/2}$, terminal half-life.
[a]Six patients at 900, 1200 and 1600 mg/day and five at 1800 mg/day.
[b]Day 1, AUC from 0 to infinity; Day 21, AUC from 0 to 24 h.

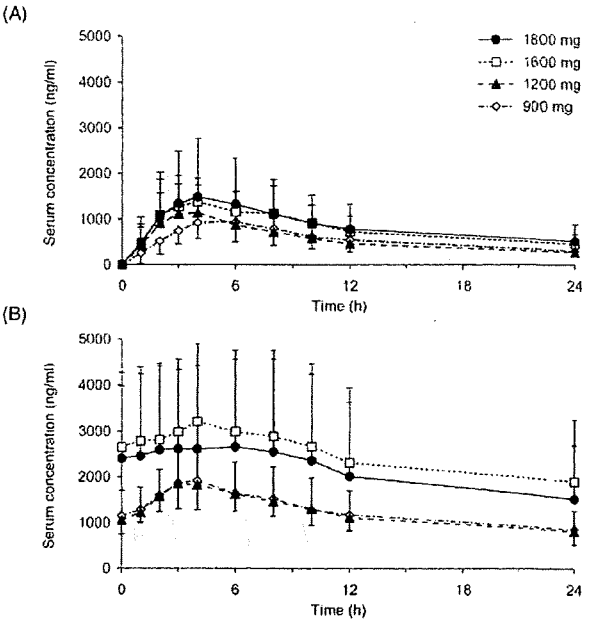

Figure 1. Serum concentrations of lapatinib at each dose level as detected on (A) Day 1 and (B) Day 21.

Steady-state serum concentrations of lapatinib generally increased with dose, 820 ± 448 ng/ml at 1200 mg dose level and 1899 ± 1356 ng/ml at 1600 mg dose level (Table 3). Both concentrations exceeded the half maximal inhibitory concentration values for *in vitro* tumor growth (14). The median $t_{1/2}$ after repeat dose was 16.9 h (range, 15.1–34.3) at 1200 mg dose level and 26.2 h (range, 12.9–48.3) at 1600 mg dose level.

The fraction of urinary excretion of lapatinib was <0.1% of the dose, suggesting that none or negligible amount of drug is excreted in urine.

Comparison of on-treatment C_{max} and AUC_{0-24} values obtained in Japanese and western patients are shown in Fig. 2 (43,44).

Efficacy

Among 24 patients, the best overall response was assessed as partial response (PR) in two patients (8.3%), stable disease (SD) in 12 patients (50.0%), progressive disease in eight patients (33.3%) and indeterminate in two patients (8.3%).

Of the two patients with PR, the first was a 73-year-old man with NSCLC (squamous cell carcinoma) with prior docetaxel and gemcitabine treatment, who received lapatinib 900 mg/day. PR was assessed by CT scan with 41% shrinkage on Day 49. Time to progression was 191 days. The second patient was a 55-year-old woman with trastuzumab-resistant breast cancer (invasive ductal carcinoma; hormone receptor-negative, ErbB-2 3+). Disease progressed after doxorubicin and cyclophosphamide/docetaxel therapy, was

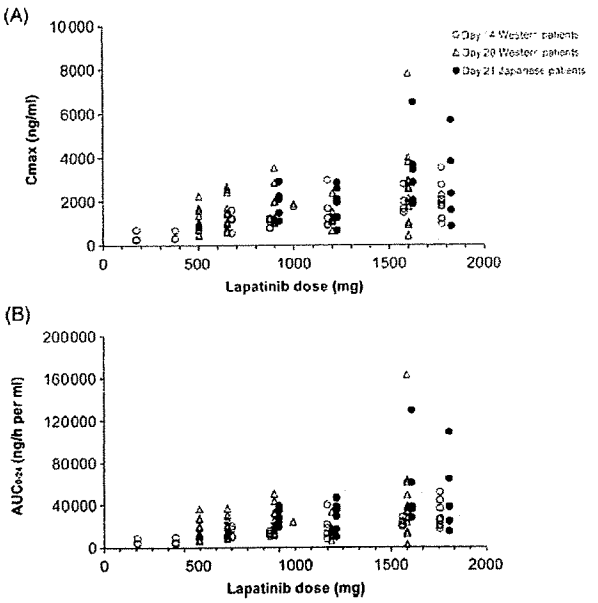

Figure 2. Relation between dose of lapatinib and exposure: comparison of (A) maximum serum concentration (C_{max}) and (B) area under the plasma drug concentration–time curve from 0 to 24 h (AUC_{0-24}) after dosing on Day 21 (our study, Japanese patients) and Days 14 and 20 (US studies, western patients).

stable with doxifluridine, and progressed with trastuzumab. Following treatment with lapatinib 1600 mg/day, the tumor shrank by 41% on Day 21. Time to progression was 133 days.

Among the patients with SD, three (two with NSCLC and one with colorectal cancer) were stabilized for >6 months and three (two with NSCLC and one with cervical cancer) were stabilized for 3–6 months and therefore were considered as having a durable response.

DISCUSSION

The dual ErbB-1/-2 inhibitor lapatinib taken orally once daily for ≥21 days was well tolerated at doses of 900–1600 mg in Japanese solid tumor patients. Adverse events were mostly mild in nature, and only four grade ≥3 drug-related adverse events were noted, in three patients (three events of Grade 3 diarrhea and one Grade 3 γ-GTP increase). No NCI-CTC Grade 4 adverse events were observed. Grade 1–2 diarrhea occurred in some patients other than those who experienced Grade 3 diarrhea; for these, supportive therapy was given and fully recovered in all cases. Grade 1/2 drug-related nausea and vomiting were experienced only by patients at higher dose levels of lapatinib, with Grade 2 symptoms only seen at 1800 mg dose level.

The types and incidences of drug-related adverse events in Japanese patients were similar to those reported from studies conducted in healthy volunteers (18) and two overseas Phase I studies, the latter including a parallel study in western patients that used similar dose administration and dose-escalation schedules (43,44). In that study as well as in ours, diarrhea and rash were the most frequently noted drug-related adverse events. Adverse events were generally mild (Grade 1–2), transient and reversible on dose delay or interruption. Headache, which was common in western patients (18), was reported only by one patient at 1600 mg dose level. 1800 mg/day was considered as MTD, at which Grade 3 diarrhea and γ-GTP increase were observed.

Skin-related adverse events of lapatinib were similar to those reported for other agents that target ErbB-1; rash is also a common adverse event associated with the ErbB-1 tyrosine kinase inhibitors gefitinib (46–49) and erlotinib (7,50), as well as the anti-ErbB-1 antibody cetuximab (51). Patients who received these medications also experienced diarrhea (7,46–50). These adverse events occurred at a similar frequency in our study as in two overseas Phase I studies (43,44).

Apart from one event of γ-GTP increase, no Grade ≥3 abnormal laboratory test suggestive of liver dysfunction was noted. Therefore, drug-related liver abnormality was generally less frequently seen with lapatinib compared with gefitinib (48,49).

Hematologic toxicity was uncommon and limited to cases of anemia. This finding is similar to those of the Phase I biomarker study (44) and studies of gefitinib (48,49,52).

None of the patients developed interstitial lung disease, which is an adverse event reportedly associated with gefitinib (53,54) and occurs in 5.8% of Japanese patients (55). However, because of the limited number of patients in our study, further studies are required to assess safety of lapatinib in this regard.

Cardiotoxicity is a known adverse event associated with trastuzumab therapy and might be related to ErbB-2 inhibition (2,56); however, we found no evidence of drug-related cardiac dysfunction in our study.

PK parameters such as C_{max} and AUC_{0-24} in this study were analyzed and their means and 95% confidence intervals compared with those obtained at similar doses (900–1800 mg) in two overseas Phase I studies (43,44). As can be seen in Fig. 2, the values were comparable among the three studies. However, large inter-patient variations were noted, especially in Japanese patients, and these might have contributed to higher mean values. On the other hand, no clear pharmacokinetic differences were apparent between Japanese and non-Japanese subjects, suggesting that values obtained overseas can be extrapolated to the Japanese population.

The dose recommended for further clinical studies outside Japan, 1500 mg/day, can be used for Phase II studies in Japan. We base this recommendation on the similar PK profiles of lapatinib in Japanese and western patients, evidence of antitumor activity at doses of ≥900 mg/day, and an MTD of 1800 mg/day.

To conclude, lapatinib, taken continuously as once-daily oral therapy at 900–1600 mg, was well tolerated in Japanese

patients with solid tumors. The safety and PK profiles shown in this study are similar to those in Phase I studies conducted in western patients. Phase II studies to determine the efficacy of lapatinib against a range of tumors are now in progress.

Acknowledgements

We thank all the patients who participated in this study, their families, and all the investigators (Dr K. Araki, Dr M. Fukuda, Dr M. Ikeda, Dr H. Kaneda, Dr T. Sato, Dr M. Tahara and Dr K. Tamura), research nurses, and study coordinators at study sites.

Funding

This study was sponsored by GlaxoSmithKline K.K.

Conflict of interest statement

The author, Hironobu Minami, receives honoraria from GlaxoSmithKline. The authors, Masayuki Kanezaki, Akihira Mukaiyama, and Yoshiyuki Minamide are employed by GlaxoSmithKline.

References

1. Yarden Y, Sliwkowski MX. Untangling the ErbB signalling network. *Nat Rev Mol Cell Biol* 2001;2:127–37.
2. Horton J. Trastuzumab use in breast cancer: clinical issues. *Cancer Control* 2002;9:499–507.
3. Sridhar SS, Seymour L, Shepherd FA. Inhibitors of epidermal-growth-factor receptors: a review of clinical research with a focus on non-small-cell lung cancer. *Lancet Oncol* 2003;4:397–406.
4. Rocha-Lima CM, Soares HP, Raez LE, Singal R. EGFR targeting of solid tumors. *Cancer Control* 2007;14:295–304.
5. Baselga J, Averbuch SD. ZD1839 ('Iressa') as an anticancer agent. *Drugs* 2000;60(Suppl. 1):33–40. Discussion 41–2.
6. Baselga J, Pfister D, Cooper MR, Cohen R, Burtness B, Bos M, et al. Phase I studies of anti-epidermal growth factor receptor chimeric antibody C225 alone and in combination with cisplatin. *J Clin Oncol* 2000;18:904–14.
7. Hidalgo M, Siu LL, Nemunaitis J, Rizzo J, Hammond LA, Takimoto C, et al. Phase I and pharmacokinetic study of OSI-774, an epidermal growth factor receptor tyrosine kinase inhibitor, in patients with advanced solid malignancies. *J Clin Oncol* 2001;19:3267–79.
8. Fry DW. Mechanism of action of erbB tyrosine kinase inhibitors. *Exp Cell Res* 2003;284:131–9.
9. Veronese ML, O'Dwyer PJ. Monoclonal antibodies in the treatment of colorectal cancer. *Eur J Cancer* 2004;40:1292–301.
10. Esteva FJ. Monoclonal antibodies, small molecules, and vaccines in the treatment of breast cancer. *Oncologist* 2004;9(Suppl. 3):4–9.
11. Simpson BJ, Phillips HA, Lessells AM, Langdon SP, Miller WR. c-erbB growth-factor-receptor proteins in ovarian tumors. *Int J Cancer* 1995;64:202–6.
12. Cohen BD, Kiener PA, Green JM, Foy L, Fell HP, Zhang K. The relationship between human epidermal growth–like factor receptor expression and cellular transformation in NIH3T3 cells. *J Biol Chem* 1996;271:30897–903.
13. Suo Z, Risberg B, Kalsson MG, Willman K, Tierens A, Skovlund E, et al. EGFR family expression in breast carcinomas. c-erbB-2 and c-erbB-4 receptors have different events on survival. *J Pathol* 2002;196:17–25.
14. Rusnak DW, Lackey K, Affleck K, Wood ER, Alligood KJ, Rhodes N, et al. The effects of the novel, reversible epidermal growth factor receptor/ErbB-2 tyrosine kinase inhibitor, GW2016, on the growth of human normal and tumor-derived cell lines *in vitro* and *in vivo*. *Mol Cancer Ther* 2001;1:85–94.
15. Xia W, Mullin RJ, Keith BR, Liu L-H, Ma H, Rusnak DW, et al. Anti-tumor activity of GW572016: a dual tyrosine kinase inhibitor blocks EGF activation of EGFR/erbB2 and downstream Erk1/2 and AKT pathways. *Oncogene* 2002;21:6255–63.
16. Wood ER, Truesdale AT, McDonald OB, Yuan D, Hassell A, Dickerson SH, et al. A unique structure for epidermal growth factor receptor bound to GW572016 (lapatinib): relationships among protein conformation, inhibitor off-rate, and receptor activity in tumor cells. *Cancer Res* 2004;64:6652–9.
17. Xia W, Liu L-H, Ho P, Spector NL. Truncated ErbB2 receptor ($p95^{ErbB2}$) is regulated by heregulin through heterodimer formation with ErbB3 yet remains sensitive to the dual EGFR/ErbB2 kinase inhibitor GW572016. *Oncogene* 2004;23:646–53.
18. Bence AK, Anderson EB, Halepota MA, Doukas MA, DeSimone PA, Davis GA, et al. Phase I pharmacokinetic studies evaluating single and multiple doses of oral GW572016, a dual EGFR–ErbB2 inhibitor, in healthy subjects. *Invest New Drugs* 2005;23:39–49.
19. Raymond E, Faivre S, Armand JP. Epidermal growth factor receptor tyrosine kinase as a target for anticancer therapy. *Drugs* 2000;60(Suppl. 1):15–23.
20. Duda RB, Cundiff D, August CZ, Wagman LD, Bauer KD. Growth factor receptor and related oncogene determination in mesenchymal tumors. *Cancer* 1993;71:3526–30.
21. Rieske P, Kordek R, Bartkowiak J, Debiec-Rychter M, Biernat W, Liberski PP. A comparative study of epidermal growth factor receptor (EGFR) and MDM2 gene amplification and protein immunoreactivity in human glioblastomas. *Pol J Pathol* 1998;49:145–9.
22. Hoffmann TK, Balló H, Braunstein S, Van Lierop A, Wagenmann M, Bier H. Serum level and tissue expression of c-erbB-1 and c-erbB-2 proto-oncogene products in patients with squamous cell carcinoma of the head and neck. *Oral Oncol* 2001;37:50–6.
23. Wang W, Johansson HE, Bergholm UI, Westermark KM, Grimelius LE. Expression of c-Myc, TGF-alpha and EGF-receptor in sporadic medullary thyroid carcinoma. *Acta Oncol* 1997;36:407–11.
24. Iihara K, Shiozaki H, Tahara H, Kobayashi K, Inoue M, Tamura S, et al. Prognostic significance of transforming growth factor-alpha in human esophageal carcinoma. Implication for the autocrine proliferation. *Cancer* 1993;71:2902–9.
25. Lee CS, Pirdas A. Epidermal growth factor receptor immunoreactivity in gallbladder and extrahepatic biliary tract tumours. *Pathol Res Pract* 1995;191:1087–91.
26. Yoshida K, Hosoya Y, Sumi S, Honda M, Moriguchi H, Yano M, et al. Studies of the expression of epidermal growth factor receptor in human renal cell carcinoma: a comparison of immunohistochemical method versus ligand binding assay. *Oncology* 1997;54:220–5.
27. Sriplakich S, Jahnson S, Karlsson MG. Epidermal growth factor receptor expression: predictive value for the outcome after cystectomy for bladder cancer? *BJU Int* 1999;83:498–503.
28. Kim JW, Kim YT, Kim DK. Correlation between EGFR and c-erbB-2 oncoprotein status and response to neoadjuvant chemotherapy in cervical carcinoma. *Yonsei Med J* 1999;40:207–14.
29. Miturski R, Semczuk A, Postawski K, Jakowicki JA. Epidermal growth factor receptor immunostaining and epidermal growth factor receptor-tyrosine kinase activity in proliferative and neoplastic human endometrium. *Tumour Biol* 2000;21:358–66.
30. Scholes AG, Hagan S, Hiscott P, Damato BE, Grierson I. Overexpression of epidermal growth factor receptor restricted to macrophages in uveal melanoma. *Arch Ophthalmol* 2001;119:373–7.
31. Beech D, Pollock RE, Tsan R, Radinsky R. Epidermal growth factor receptor and insulin-like growth factor-I receptor expression and function in human soft-tissue sarcoma cells. *Int J Oncol* 1998;12:329–36.
32. Oda Y, Wehrmann B, Radig K, Walter H, Röse I, Neumann W, et al. Expression of growth factors and their receptors in human osteosarcomas. Immunohistochemical detection of epidermal growth factor, platelet-derived growth factor and their receptors: its correlation with proliferating activities and p53 expression. *Gen Diagn Pathol* 1995;141:97–103.

33. Koeppen HK, Wright BD, Burt AD, Quirke P, McNicol AM, Dybdal NO, et al. Overexpression of HER2/neu in solid tumours: an immunohistochemical survey. *Histopathology* 2001;38: 96–104.
34. Press MF, Pike MC, Hung G, Zhou JY, Ma Y, George J, et al. Amplification and overexpression of HER-2/neu in carcinomas of the salivary gland: correlation with poor prognosis. *Cancer Res* 1994;54:5675–82.
35. Haugen DR, Akslen LA, Varhaug JE, Lillehaug JR. Expression of c-erbB-2 protein in papillary thyroid carcinomas. *Br J Cancer* 1992;65:832–7.
36. Lam KY, Tin L, Ma L. C-erbB-2 protein expression in oesophageal squamous epithelium from oesophageal squamous cell carcinomas, with special reference to histological grade of carcinoma and pre-invasive lesions. *Eur J Surg Oncol* 1998;24:431–5.
37. Herrera GA. C-erb B-2 amplification in cystic renal disease. *Kidney Int* 1991;40:509–13.
38. Rolitsky CD, Theil KS, McGaughy VR, Copeland LJ, Niemann TH. HER-2/neu amplification and overexpression in endometrial carcinoma. *Int J Gynecol Pathol* 1999;18:138–43.
39. Leng J, Lang J, Shen K, Guo L. Overexpression of p53, EGFR, c-erbB2 and c-erbB3 in endometrioid carcinoma of the ovary. *Chin Med Sci J* 1997;12:67–70.
40. Foster H, Ganti AK, Knox S, Hebert B, Tendulkar K, Fraiman GN, et al. Determination and role of HER-2/neu overexpression in soft tissue sarcomas. *Proc Am Soc Clin Oncol* 2002;21: (Abstract 1622).
41. World Medical Association. World Medical Association Declaration of Helsinki. 2004. Available at: http://www.wma.net/e/policy/b3.htm.
42. Japan Ministry of Health and Welfare. Good clinical practice for trials on drugs. Ordinance no. 28. Tokyo, Japan Ministry of Health and Welfare 1997.
43. Versola M, Burris HA, Jones S, Wilding G, Taylor C, Pandite L, et al. Clinical activity of GW572016 in EGF10003 in patients with solid tumors. *Proc Am Soc Clin Oncol* 2004;23: (Abstract 3047).
44. Burris HA, III, Hurwitz HI, Dees EC, Dowlati A, Blackwell KL, O'Neil B, et al. Phase I safety, pharmacokinetics, and clinical activity study of lapatinib (GW572016), a reversible dual inhibitor of epidermal growth factor receptor tyrosine kinases, in heavily pretreated patients with metastatic carcinomas. *J Clin Oncol* 2005;23:5305–13.
45. Therasse P, Arbuck SG, Eisenhauer EA, Wanders J, Kaplan RS, Rubinstein L, et al. New guidelines to evaluate the response to treatment in solid tumors. European Organization for Research and Treatment of Cancer, National Cancer Institute of the United States, National Cancer Institute of Canada. *J Natl Cancer Inst* 2000;92:205–16.
46. Baselga J, Rischin D, Ranson M, Calvert H, Raymond E, Kieback DG, et al. Phase I safety, pharmacokinetic, and pharmacodynamic trial of ZD1839, a selective oral epidermal growth factor receptor tyrosine kinase inhibitor, in patients with five selected tumor types. *J Clin Oncol* 2002;20:4292–302.
47. Herbst RS, Maddox A-M, Rothenberg ML, Small EJ, Rubin EH, Baselga J, et al. Selective oral epidermal growth factor receptor tyrosine kinase inhibitor ZD1839 is generally well-tolerated and has activity in non-small-cell lung cancer and other solid tumors: results of a phase I trial. *J Clin Oncol* 2002;20:3815–25.
48. Fukuoka M, Yano S, Giaccone G, Tamura T, Nakagawa K, Douillard J-Y, et al. Multi-institutional randomized phase II trial of gefitinib for previously treated patients with advanced non-small-cell lung cancer (the IDEAL 1 trial). *J Clin Oncol* 2003;21:2237–46.
49. Nakagawa K, Tamura T, Negoro S, Kudoh S, Yamamoto N, Yamamoto N, et al. Phase I pharmacokinetic trial of the selective oral epidermal growth factor receptor tyrosine kinase inhibitor gefitinib ('Iressa', ZD1839) in Japanese patients with solid malignant tumors. *Ann Oncol* 2003;14:922–30.
50. Yamamoto N, Horiike A, Fujisaka Y, Murakami H, Shimoyama T, Yamada Y, et al. Phase I dose-finding and pharmacokinetic study of the oral epidermal growth factor receptor tyrosine kinase inhibitor Ro50-8231 (erlotinib) in Japanese patients with solid tumors. *Cancer Chemother Pharmacol* 2008;61:489–96.
51. Busam KJ, Capodieci P, Motzer R, Kiehn T, Phelan D, Halpern AC. Cutaneous side-events in cancer patients treated with the antiepidermal growth factor receptor antibody C225. *Br J Dermatol* 2001;144: 1169–76.
52. Ranson M, Hammond LA, Ferry D, Kris M, Tullo A, Murray PI, et al. ZD1839, a selective oral epidermal growth factor receptor-tyrosine kinase inhibitor, is well tolerated and active in patients with solid malignant tumors: results of a phase I trial. *J Clin Oncol* 2002;20:2240–50.
53. Inoue A, Saijo Y, Maemondo M, Gomi K, Tokue Y, Kimura Y, et al. Severe acute interstitial pneumonia and gefitinib. *Lancet* 2003;361:137–9.
54. Takano T, Ohe Y, Kusumoto M, Tateishi U, Yamamoto S, Nokihara H, et al. Risk factors for interstitial lung disease and predictive factors for tumor response in patients with advanced non-small cell lung cancer treated with gefitinib. *Lung Cancer* 2004;45:93–104.
55. Yoshida S. The results of gefitinib prospective investigation. *Med Drug J* 2005;41:772–89.
56. Suter TM, Cook-Burns N, Barton C. Cardiotoxicity associated with trastuzumab (Herceptin) therapy in the treatment of metastatic breast cancer. *Breast* 2004;13:173–83.

Biomarkers, 2009; 14(7): 529–538

informa
healthcare

ORIGINAL ARTICLE

MicroRNA-500 as a potential diagnostic marker for hepatocellular carcinoma

Yusuke Yamamoto[1,2], Nobuyoshi Kosaka[1,2], Minoru Tanaka[3], Fumiaki Koizumi[4], Yae Kanai[5], Takayuki Mizutani[6], Yoshiki Murakami[7], Masahiko Kuroda[8], Atsushi Miyajima[3], Takashi Kato[2], and Takahiro Ochiya[1,2]

[1]Section for Studies on Metastasis, [4]Genetics Division and [5]Pathology Division, National Cancer Center Research Institute, 1-1, Tsukiji, 5-chome, Chuo-ku, Tokyo 104-0045, Japan, [2]Major in Integrative Bioscience and Biomedical Engineering, Graduate School of Science and Engineering, Waseda University, Nishi-Waseda 1-6-1, Shinjuku-ku, Tokyo, 169-8050, Japan, [3]Laboratory of Cell Growth and Differentiation, Institute of Molecular and Cellular Biosciences, University of Tokyo, Yayoi, Bunkyo-ku, Tokyo 113-0032, Japan, [6]B-Bridge International, Inc., 320 Logue Ave. Mountain View, CA 94043, USA, [7]Center for Genomic Medicine, Kyoto University Graduate School of Medicine, Shogoinkawaharacho 53, Sakyo-ku, Kyoto 606-8507, Japan, and [8]Tokyo Medical University, 6-1-1, Shinjuku, Shinjyuku-ku, Tokyo 160-8402, Japan

Abstract

We identified that microRNA expression changed dynamically during liver development and found that miR-500 is an oncofetal miRNA in liver cancer. miR-500 was abundantly expressed in several human liver cancer cell lines and 45% of human hepatocellular carcinoma (HCC) tissue. Most importantly, an increased amount of miR-500 was found in the sera of the HCC patients. In fact, miR-500 levels in sera of the HCC patients returned to normal after the surgical treatment in three HCC patients. Our findings reveal that diverse changes of miRNAs occur during liver development and, one of these, miR-500 is an oncofetal miRNA relevant to the diagnosis of human HCC.

Keywords: *miRNA; miR-500; hepatocellular carcinoma, liver development, diagnosis*

Introduction

MicroRNAs (miRNAs) are small RNA molecules of 21–25 nt that have the potential to a play central role in physiological and pathological processes, including cell differentiation, apoptosis and oncogenesis (Ambros 2004, Esquela-Kerscher et al. 2006). The biogenesis of miRNAs involves nucleolytic processing of precursor transcripts, which are transcribed from different genomic locations as long primary transcripts (pri-miRNA) by RNA polymerase II in the nucleus (Lee et al. 2004). Pri-miRNAs are processed by the RNase-III family of an enzyme, Drosha, to a ~70 nt precursor called the pre-miRNA. The pre-miRNA is exported to the cytoplasm by Exportin-5 and then cleaved in the cytoplasm by Dicer to ~22 nt double-strand mature miRNA (Han et al. 2006, Lund et al. 2004, Ketting et al. 2001). A single strand of the mature miRNA is assembled into effecter complexes called miRNPs (miRNA-containing ribonucleoprotein particles), which share a considerable amount of similarity with an RNA-induced silencing complex (RISC) (Nelson et al. 2004). They induce gene suppression post-transcriptionally by inducing mRNA degradation or by regulating the translational efficiency of mRNA (Bartel 2004).

Several reports have shown the importance of miRNA functions in tissue development. More recent reports, in particular those regarding comprehensive microRNA profiling analysis, have shown that miRNAs are expressed in a tissue-specific manner and their expression altered

Address for Correspondence: Takahiro Ochiya, Section for Studies on Metastasis, National Cancer Center Research Institute, 1-1, Tsukiji, 5-chome, Chuo-ku, Tokyo 104-0045, Japan. Tel: +81-3-3542-2511, ext. 4800. Fax: +81-3-3541-2685. E-mail: tochiya@ncc.go.jp

(Received 19 May 2009; revised 29 June 2009; accepted 29 June 2009)

ISSN 1354-750X print/ISSN 1366-5804 online © 2009 Informa UK Ltd
DOI: 10.3109/13547500903150771

in the process of development, such as cardiogenesis and haematopoiesis (Chen et al. 2006, 2004). For example, miR-1, which is expressed specifically in cardiac and skeletal muscle, is essential for cardiac morphogenesis and conduction (Zhao et al. 2007). Another study showed that miR-181a regulates intrinsic antigen sensitivity during T-cell development (Li et al. 2007). Another important aspect of miRNA study is the association of its gene targets and disease, which have been investigated by many researchers. Mir-17-92 polycistron has been designated as oncomiR-1 (He et al. 2005), and let-7 family miRNAs and miR-34 function as tumour suppressors (Johnson et al. 2005, Yu F et al. 2007, He et al. 2007); moreover, a number of studies have given evidence that several miRNAs are associated with carcinogenesis and regulate the expression of cancer-related genes.

Although emerging evidence suggests that several miRNAs are involved in the process of liver development (Esau et al. 2006, Fu et al. 2005, Gramantieri et al. 2007), the roles of miRNAs in hepatogenesis and their possible relation to hepatocarcinogenesis have not been thoroughly examined. In this study, to investigate liver development from the biological aspects of microRNA, we performed a mouse miRNA microarray carrying 340 miRNA probes. We report that some of these miRNAs are strongly expressed, and that dynamic changes in their expression profile are observed in the process of liver development. We also show that miR-500 is an oncofetal miRNA, which is highly expressed in fetal liver, more than in adult normal liver, and aberrantly expressed in hepatocellular carcinoma (HCC) tissue. Thus, dynamic miRNA regulation is an important feature as an oncofetal non-coding small RNA relevant to the diagnosis of human liver cancer.

Materials and methods

RNA extraction

C57BL/6J mice were used in this study. Total RNA from mouse liver tissues (embryo (E) 14, E16, E18, neonate and adult), *in vitro* fetal hepatocyte cultured samples (days 0, 1, 3, 5 and 7), and liver cancer cell lines (HepG2, Huh-7, JHH-7, Alexander, Li-7, and Hep3B) were extracted using the mirVana™ miRNA Isolation Kit (Ambion, Tokyo, Japan). Animal experiments in the present study were performed in compliance with the guidelines of the Institute for Laboratory Animal Research, National Cancer Center Research Institute.

Locked nucleic acid (LNA)-based miRNA microarray

The miRCURY™ LNA array version 8.0, which contains capture probes targeting all human, mouse and rat miRNA listed in the miRBASE version 8.0, was applied to detect the expression of mouse miRNA (Exiqon, Vedbaek, Denmark). Total RNA samples were collected from fetal (E14, 16 and 18), neonate and adult (8-week-old) mice ($n=7$–10). Total RNA samples (2000 ng) from liver tissue and reference (Universal control, which is made from mouse tissue mixtures) were labelled with the Hy3™ and Hy5™ fluorescent stain, respectively, using the miRCURY™ LNA Array labelling kit according to the procedure described by the manufacturer (Exiqon). Hybridisation and normalisation were performed according to the miRCURY™ LNA array manual, and image analysis of the miRCURY™ LNA array microarray slides was acquired using an Agilent Technologies Microarray Scanner and Agilent Feature Extraction 9.1 (Agilent Technologies, Tokyo, Japan). A hierarchical cluster was produced from microarray data using a Euclidean distance calculation based on Ward's methods by GenMaths software (Applied Maths). All the miRNA microarray data are shown in Supplementary Table 1 (see the online version of this article).

Cell culture

Liver cancer cell lines (HepG2, Huh-7, JHH-7, Alexander, Li-7 and Hep3B) were cultured in liquid culture with Dulbecco's modified eagle medium (DMEM; GIBCO Laboratories, Grand Island, NY, USA) supplemented with heat-inactivated 10% fetal bovine serum (FBS; Equitech-Bio, Kerrville, TX, USA) and a 1% antibiotic antimycotic solution (Invitrogen, Tokyo, Japan). The cells were maintained *in vitro* at 37°C in a humidified atmosphere with 5% CO_2.

Patients and RNA specimens

Liver tissues were obtained surgically with informed consent from patients at the National Cancer Center Hospital (Tokyo, Japan). The study was approved by the Institutional Review Board of the National Cancer Center Research Institute. Liver tissue total RNAs were extracted from 40 HCC patients and their associated non-cancerous tissue. The clinical data and pathological diagnosis are summarized in Supplementary Table 2 (see the online version of this article).

Real-time polymerase chain reaction

Total RNAs of approximately 100 ng were reverse-transcribed using the Taqman miRNA reverse transcription kit (Applied Biosystems, Tokyo, Japan). Real-time quantitative polymerase chain reaction (PCR) amplification of the cDNA template was done using Taqman Universal PCR Master Mix (Applied Biosystems) in

an ABI PRISM 7300 (Applied Biosystems). The PCR conditions were 50°C for 2 min and 95°C for 10 min followed by 50 cycles of 95°C for 15 s and 60°C for 1 min. Taqman probes for human and mouse miRNA were used to assess the expression levels of miRNA (mmu-miR-101b, ID 4373159; mmu-122a, ID 4373151; mmu-miR-142-5p, ID 4373135; mmu-miR-223, ID 4373075; mmu-miR-451, ID 4373360; has-miR-346, ID 4373038; has-miR-500, ID 4373225; Applied Biosystems). The expression levels were normalised against U6 (RNU6B, ID 4373381; Applied Biosystems) or total RNA volume.

RNA isolation from human serum samples

Whole blood samples were obtained from patients with HCC at the Kyoto University (Kyoto, Japan). All of the donors or their guardians provided written consent and ethics permission was obtained for the use of all samples. Blood samples were taken before and after completion of surgery. Serum samples were stored at -80°C until analysis. For serum RNA isolation, total RNA was isolated using Isogen (Nippon Gene, Japan), according to the manufacturer's instructions.

Measurement of serum miRNA levels by using TaqMan qRT-PCR assays

A fixed volume of 5 µl of RNA solution (14 ng) was used as input into the reverse transcription reaction. Input RNA was reverse transcribed using the TaqMan miRNA Reverse Transcription Kit and miRNA-specific stem-loop primers (Applied BioSystems) in a small-scale reverse transcription reaction (comprising 2 µl of H_2O, 1 µl of 10x reverse-transcription buffer, 0.2 µl of RNase inhibitor (20 units ml^{-1}), 0.1 µl of 100 mM dNTPs, 0.7 µl of Multiscribe reverse transcriptase and 5 µl of input RNA), using a Tetrad2 Peltier Thermal Cycler (BioRad, Tokyo, Japan) at 16°C for 30 min, 42°C for 30 min and 85°C for 5 min. Teverse transcription product (4.75 µl) was combined with 5.25 µl of PCR assay reagents (comprising 5 µl of TaqMan 2x Universal PCR Master Mix, No AmpErase UNG and 0.25 µl of TaqMan miRNA assay) to generate a PCR of 10.0 µl of total volume. Real-time PCR was performed as described above. Serum levels of miR-16 were measured as internal normalisation control as they were not significantly different between controls and patients in prostate cancer and colorectal cancer (Mitchell et al. 2008).

Statistical analysis

The results are given as mean ± SD. The Student's *t*-test was performed for statistical evaluation; $p < 0.05$ or $p < 0.001$ was considered significant.

Table 1. MicroRNAs (miRNA) abundantly expressed in liver development.

Liver stage	MiRNA name[a]
E14	miR-122a, miR-142-3p, miR-142-5p, miR-144, miR-223, miR-346, miR-374-5p, miR-451, miR-486, miR-500
E16	miR-101b, miR-122a, miR-142-3p, miR-142-5p, miR-144, miR-223, miR-295, miR-346, miR-367, miR-374-5p, miR-451, miR-464, miR-471, miR-486, miR-500, miR-547
E18	miR-101b, miR-122a, miR-142-3p, miR-142-5p, miR-144, miR-223, miR-324-3p, miR-374-5p, miR-451, miR-486
Neonate	miR-101b, miR-122a, miR-142-3p, miR-142-5p, miR-144, miR-223, miR-463
Adult	miR-21, miR-22, miR-29a, miR-29b, miR-29c, miR-101a, miR-101b, miR-122a, miR-126-5p, miR-192, miR-374-5p

[a]miRNAs are listed in ascending order. E, embryo.

Results

Analysis of the global expression levels of miRNA in the process of liver development by LNA-based miRNA microarray

To examine how the expression profile of miRNA changed in the process of mouse liver development, we performed an LNA-based miRNA microarray at different developmental stages. Total RNAs from E14, 16, 18, neonate and adult liver were isolated and labelled with Hy3, and total RNAs of universal control consisted of several tissue mixtures labelled with Hy5 as a common reference. After normalisation of the miRNA expression, the number of high- and low-expressed miRNAs at different time stages was counted. High-expressed miRNA represents twofold or more upregulated miRNA, and low-expressed miRNA represents twofold or more downregulated miRNA, when compared with an average expression level of all miRNAs (see Supplementary Figure 1 in the online version of this article). Throughout all developmental stages of the liver, most of the miRNA expression levels were classified as low-expressed miRNA; in contrast, the number of high-expressed miRNAs was quite limited and are listed in Table 1. These data indicated that expression levels of the general miRNAs were very low and that a limited number of miRNAs were highly expressed in mouse liver development.

Differential expression patterns of miRNAs in the process of mouse liver development

To determine differentially expressed miRNA and to quantify the expression changes in the process of liver

development, hierarchical unsupervised clustering analysis was performed using microarray data of E14, 16, 18, neonate and adult mouse liver. The case cluster analysis of the microarray data indicated a similarity of clusters from the viewpoint of the expression pattern between E14 and E16 fetal liver and between neonate and adult liver (Figure 1), indicating that the miRNA expressions changed depending on the developmental stage. These results indicated that expression of most of the miRNAs was regulated precisely in the process of liver development.

The expression pattern of miRNA selected from highly expressed miRNAs (Table 1) was verified by real-time PCR to show the accuracy of miRNA expression acquired from the microarray analysis. The left panels of Figure 2 present the results of microarray analysis for five miRNAs (miR-101b, miR-122a, miR-142-5p, miR-223 and miR-451). Expressions of miR-101b and miR-122a were low at the early stage of liver development and were upregulated during maturation. In contrast, expressions of miR-142-5p, miR-223 and miR-451 were high at the early stage of liver development and were already known as miRNAs expressed in haematopoietic cells (Chen et al. 2004, Zhan et al 2007, Johnnidis et al 2008). The right panels of Figure 2 are the results of real-time PCR for the same set of miRNAs. In comparison to the microarray results and the real-time PCR results, these data obtained from two different methods showed approximately similar expression patterns of miRNAs, confirming the validity of our microarray analysis.

Interestingly, miRNAs (miR-142-5p, miR-451 and miR-223) expressed in haematopoietic cells were highly expressed at the early stages (E14 and E16) and then gradually downregulated in the process of liver development (Figure 2). Because whole fetal liver is a haematopoietic organ and a large number of haematopoietic cells are contained there, this also indicated the accuracy of expression profiling of miRNA in the process of liver development by LNA-based microarray.

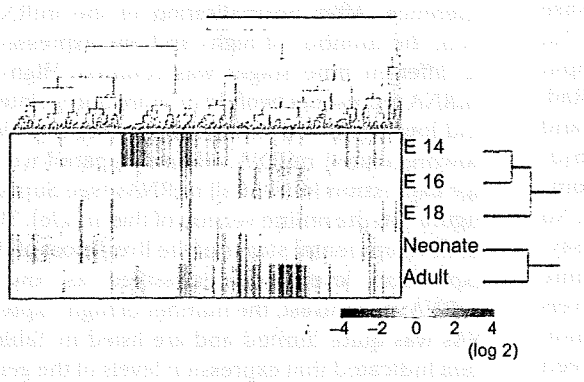

Figure 1. A global expression pattern of miRNA in the process of mouse liver development. The data were subjected to a hierarchical cluster analysis using a Euclidean distance calculation based on Ward's methods. The liver samples are aligned vertically: embryo (E) 14, E16, E18, neonate and adult. Samples were linked by the dendrogram shown on the right to highlight the similarity in their miRNA expression patterns. The expression profile of each miRNA is depicted in the respective row. The expressions of miRNA are linked by the dendrogram shown on the top to highlight the similarity in their expression patterns.

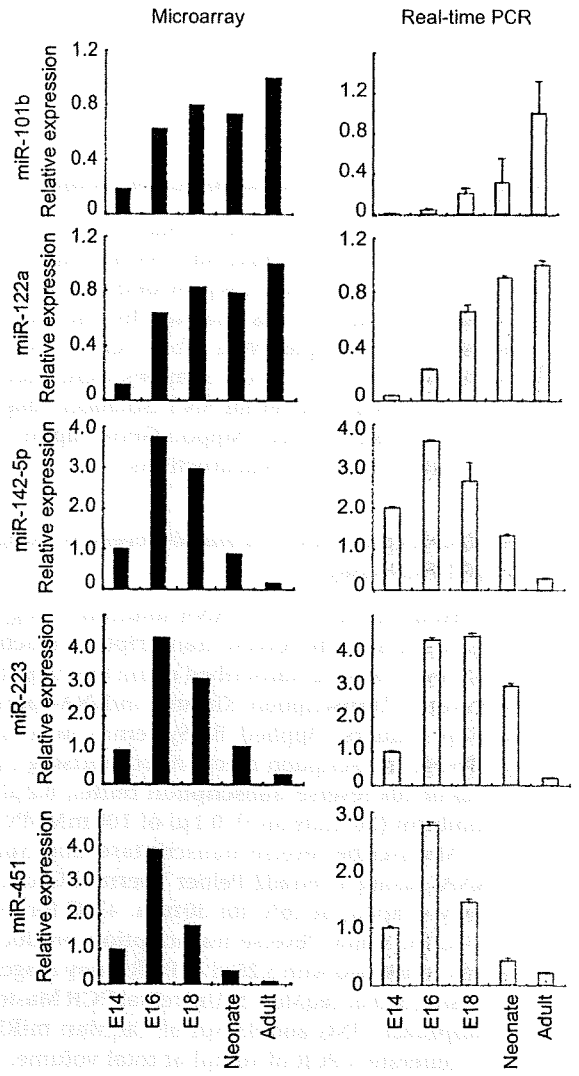

Figure 2. Differential expression of selected miRNA in mouse liver development by microarray and real-time polymerase chain reaction (PCR). miR-101b, miR-122a, miR-142-5p, miR-223 and miR-451 were selected from highly expressed miRNAs to confirm the expression levels of microarray analysis by real-time PCR. The left panels represent the miRNA expression levels by microarray analysis. The right panels represent the miRNA expression levels by real-time PCR. The expression profile is compared for mouse fetal (embryo (E) 14, E16 and E18), neonate and adult liver. In the graphs of miR-142-5p, miR-223 and miR-451, the expression level of E14 fetal liver is set to 1.0. Real-time PCR analyses were performed in triplicate and expression values are normalized with total RNA volume. Data are shown as mean ± SD.

Differential expression patterns of cancer-related miRNAs in the process of mouse liver development

Interestingly, when analysing the expression patterns of the hierarchical clustering data in detail, we found that the expression of several let-7 miRNA family known as 'tumour suppressor miRNA' was upregulated, and, in contrast, the expression of miRNAs known as 'potential oncogenes' which are involved in cell proliferation, was downregulated in the process of liver development. Therefore, to reveal the expression pattern of cancer-related miRNAs in the process of mouse liver development, the expression profile of 21 selected miRNAs (11 miRNAs as oncogenes and 10 miRNAs as tumour suppressors) is summarized in Figure 3. Many oncogenic miRNA expressions, such as those of miR-17-5p, miR-20, and miR-92, tended to decrease in the process of mouse liver development (Figure 3A). In contrast, except for let-7d* and let-7e, the expression pattern of the let-7 miRNA family was elevated in the process of liver development (Figure 3B). This study provides evidence that the expression of oncogenic miRNA is downregulated and that the expression of tumour suppressor miRNA is upregulated in the process of liver development.

Expression of miR-500 is high in human fetal liver

As reported above, the expression levels of oncogenic miRNAs were downregulated in liver development. We tried to identify new miRNA candidates that act as an oncogenic miRNA in the liver from the microarray data. As a first step toward the elucidation of the role of miRNAs in liver carcinogenesis, we focused on downregulated miRNAs during liver maturation, which are possibly related to cell proliferation; high expressions of miR-140, miR-346, miR-411, miR-470 and miR-500 were detected at an early stage (E14) of liver development and downregulated at the late developmental stages (E16 and E18) (Figure 4A). Among these, miR-500 and miR-346 expressions were remarkably downregulated during development; thus, we concentrated on miR-500 and miR-346, which could be expected to be a potential target relevant to fetal liver development to control the time and spatial expression of sets of mRNA.

In the next step, the occurrence of miR-500 and miR-346 was assessed in human fetal and adult liver. Real-time PCR analysis revealed that the expression of miR-500 in human fetal liver, but not that of miR-346, was significantly higher than that in normal adult liver (Figure 4B and Supplementary Figure 2A (see online version of this article)). Taken together, as miR-500 expression was downregulated in human adult liver, our data suggest that miR-500 is developmentally associated with human fetal hepatocyte specification and functions. The

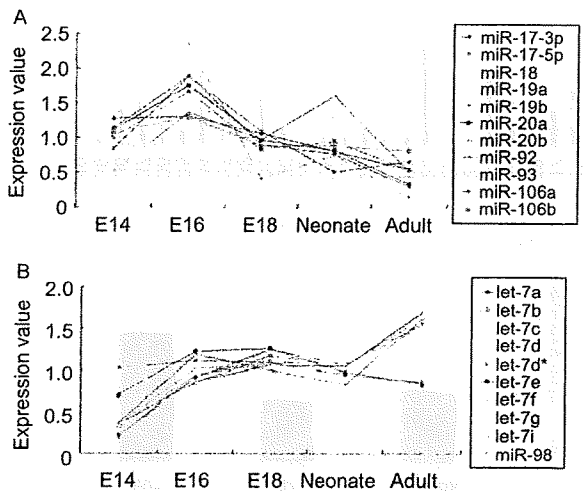

Figure 3. Expression patterns of cancer-related miRNAs in the process of mouse liver development. (A) Expression pattern by a microarray analysis (each sample: n=7-10) of miRNA that may act as an oncogene. (B) The expression pattern by the microarray analysis (each sample: n=7-10) of the let-7 family miRNAs functioned as a tumour suppressor. Expression levels are normalised by average expression value of each miRNA and shown in the graph.

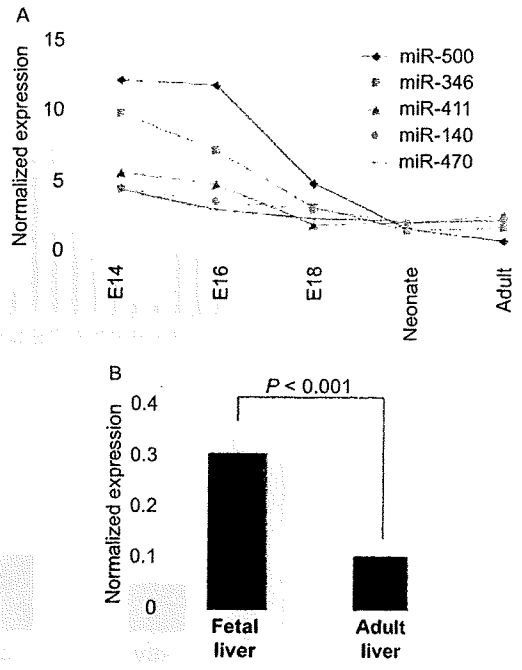

Figure 4. The expression of miR-500 is higher in the fetal stage than in the adult stage (A). The expression profile of miRNA decreased in the process of mouse liver development. Expression values are based on microarray data. (B) Expression of miR-500 in human fetal and adult liver. Real-time polymerase chain reaction analyses were performed in triplicate. Expression values are normalised with U6 snRNA value. The data represent the mean ± SD, $p < 0.001$.

results of our ongoing knock-down analysis of miRNA in liver cancer cells will be presented in a future work.

Expression of miR-500 is high in human liver cancer

We next examined the expression level of miR-500 in six human liver cancer cell lines (JHH-7, Li-7, Huh-7, HepG2, Hep3B and Alexander) to assess whether miR-500 acts as an oncofetal miRNA and found that it increases 2.4- to 47.6-fold more in Alexander, JHH-7, HepG2, Huh-7 and Hep3B than in normal liver (Figure 5A); in contrast, no detectable amount of miR-500 was found in Li-7. On the other hand, the expression levels of miR-346 in the six liver cancer cell lines were not high (see Supplementary Figure 2B in the online version of this article). To evaluate the potential of miR-500 as an oncofetal miRNA, the expression levels of human miR-500 were analysed by real-time PCR in 40 pairs of malignant neoplasias of hepatocyte lineage (T) and adjacent non-tumorous tissue (NT). Differences in the miR-500 expression level were statistically significant ($p<0.001$) between T and NT (Figure 5B), but miR-346 expression was not significantly changed (see Supplementary Figure 2C in the online version of this article). Some of the samples exhibited remarkably high expression levels of miR-500, and 45% (18/40 patients) of the samples showed 1.2- to 8.6-fold higher upregulation in the cancerous samples than in each non-tumorous sample and

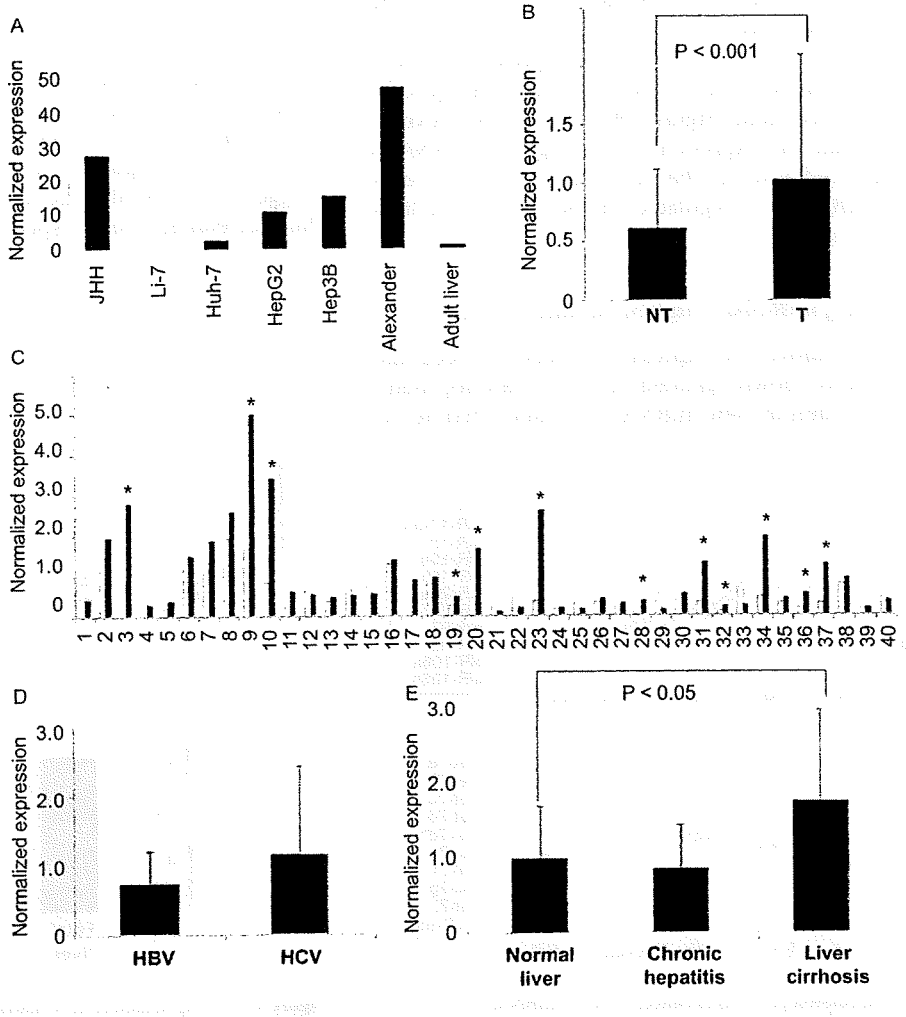

Figure 5. The expression of miR-500 is clearly upregulated in human liver cancer (A) miR-500 expression abundantly detected in liver cancer cell lines (JHH-7, Li-7, Huh-7, HepG2, Hep3B and Alexander). The expression level of normal liver is set to 1.0. The data represent the mean ± SD. (B) Forty pairs of hepatocellular carcinoma (HCC) patients (tumour (T) and non-tumour (NT)) were analysed by real-time polymerase chain reaction of human miR-500. The data represent the mean ± SD, $p<0.001$. (C) Expression levels of miR-500 in each patient (T and NT). Samples of 12 patients (*) showed twofold or more upregulation in HCC. (D) Expression levels of miR-500 in hepatitis B virus (HBV, $n=10$) and hepatitis C virus (HCV, $n=26$). (E) miR-500 expression was upregulated in liver cirrhosis ($n=17$) more than normal liver ($n=11$) and chronic hepatitis samples ($n=19$). The data represent the mean ± SD, $p<0.05$. Expression values are normalised with U6 snRNA value.

12 patients showed more than 2.0-fold higher expression (30%) (Figure 5C). Based on the clinical data and pathological diagnosis (see Supplementary Table 2 in the online version of this article), there is no significant difference in miR-500 expression between hepatitis virus B and C infection (Figure 5D). Importantly, significant difference in miR-500 expression was found between normal liver and liver cirrhosis samples, but not chronic hepatitis (Figure 5E), suggesting that miR-500 expression was upregulated during cirrhosis development. Thus, although only limited samples expressed miR-500 higher, miR-500 might be useful as a biomarker in the early stage of liver cancer.

Expression profiling of miR-500 in HCC patient serum

Recently, it has been reported that miRNAs are circulating in serum (Chim et al. 2008, Gilad et al. 2008) and tumour-derived miRNAs such as miR-155, miR-21, miR-15b, miR-16 and miR-24 are detected in the plasma and serum of tumour patients (Mitchell et al. 2008, Lawrie et al. 2008). In fact, an increased amount of miR-500 was found in the sera of three out of ten HCC patients, which means that liver cancer-specific miRNA such as miR-500 is circulating in the peripheral blood and can be a novel diagnostic marker. To determine whether or not serum levels of miR-500 truly reflect the presence of cancer in the HCC patients, the presence of miR-500 in the sera of three human HCC patients, post- and presurgical treatment, was also assessed. As can be seen in Figure 6, elevated serum levels of miR-500 in the three HCC patients were significantly reduced after surgery and returned to normal levels. These results expect that the miR-500s abundance profile in serum of the HCC patients might reflect physiological and/or pathological conditions.

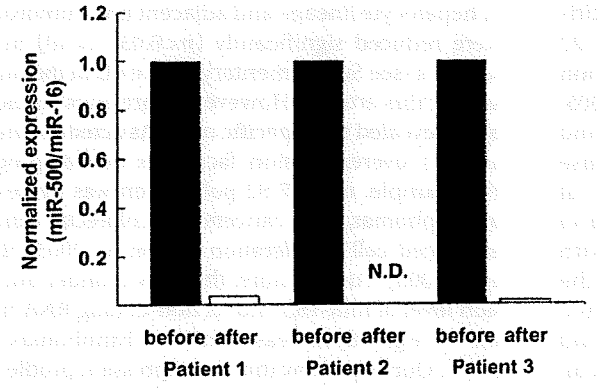

Figure 6. Serum levels of miR-500 in hepatocellular carcinoma (HCC) patients. Changes of serum levels of miR-500 in HCC patients ($n=3$) before (preoperation) and after (postoperation within 6 months) surgical removal of the tumour. Expression levels of the miR-500 are normalised to miR-16. N.D., not detected.

Discussion

Using a global miRNA expression profile in mouse liver development analysed by an LNA-based miRNA microarray, our data indicate that dynamic changes in miRNA expression occur in mouse liver development. However, the number of high-expressed miRNAs was quite limited at all developmental stages of the liver. This finding is also consistent with several reports that dominant miRNA expression is rigidly controlled in a developmental stage-specific and tissue- or cell-type-specific manner (Chen et al 2006, Shan et al. 2007). For example, it has been reported that the expressions of miR-1 and miR-133 are high and specific in adult cardiac and skeletal muscles and modulate skeletal muscle proliferation and differentiation by negatively regulating the histone deacetylase-4 or serum response factor (Chen et al. 2006). On the other hand, expression levels of the general miRNA are low at all stages of liver development. However, our data indicate that the expression pattern of some of the low-expressed miRNAs, including let-7 family, also dramatically change in the process of mouse liver development (Figure 4B). Using this platform, the overall regulation of individual miRNAs of sequential stages of liver development was determined, providing us with a useful baseline for understanding the developmental dynamics of liver miRNA expression.

In this study, we identified a novel cancer biomarker candidate, miR-500, which was designated as an oncofetal miRNA in the early stage of liver cancer, because miR-500 expression is highly expressed in a fetal liver and downregulated in the developmental process and then upregulated in the process of liver cirrhosis. When the expression profile of miR-500 in human tissues was examined, its expression was not specific in the liver and was broadly detected in all tissues (see Supplementary Figure 3 in the online version of this article). However, the expression level of miR-500 is high at the early stages of liver development in mice and humans. Furthermore, miR-500 was abundantly expressed in human liver cancer cell lines (JHH-7, Huh-7, HepG2, Hep3B and Alexander) and liver cancer tissues. Interestingly, six miRNAs (mir-532, 188, 362, 501, 660, 502) in addition to miR-500 make a cluster within a 10-kb distance from miR-500, and their expressions could be modulated by the same transcriptional regulatory unit. However, the levels were not remarkably changed during mouse liver development. Therefore, by analysing these miRNAs together, miR-500 might be a better biomarker in HCC.

We tried to test the effect of miR-500 using liver cancer cell lines. In a knock-down analysis of miR-500 with miR-500 LNA, significant changes in cell proliferation and colony formation were not observed in both Alexander and JHH-7 cells (see Supplementary Figure 5A and B in the online version of this article). Likewise, mature

miR-500 were transfected into Li-7 cells, which did not express miR-500 and we found there are no significant differences in cell proliferation (see Supplementary Figure 5C in the online version of this article). Although our data indicated that miR-500 did not affect cell proliferation in liver cancer cell lines, there might be a close association between tissue development and carcinogenesis in the fields of miRNA. For detailed analysis of function of miR-500, we await for generation of miR-500 knockout mice.

As several groups have reported that levels of certain circulating miRNA are associated with clinical characteristics in diseases (Gilad et al. 2008, Lawrie et al. 2008), our data suggest that miR-500 was circulating in the sera of the HCC patients and miR-500 levels in sera of the HCC patients returned to normal after the surgery. Although our results are promising for miRNA-based HCC screening, there are several limitations in this study and we suggest: (1) as the sample size is quite small, further validation that miR-500 could be a reliable marker for HCC in a large cohort is necessary; (2) use of better controls to determine whether or not serum miR-500 levels are changed due to the trauma of surgery; (3) it is desirable to examine whether serum miR-500 levels change in patients with chronic hepatitis and liver cirrhosis; (4) it is necessary to compare if serum miR-500 could be better than earlier diagnostic methods such as serum α-fetoprotein.

The differential expression patterns of miR-101b, miR-122a, miR-142-5p, miR-223 and miR-451 were determined by miRNA microarray and real-time PCR analysis. The specific expression of miR-122 in the liver has previously been described by several research groups. Esau et al. (2006) reported that miR-122 was a key regulator of lipid metabolism in the liver, regulating increased hepatic fatty acid oxidation, a decrease in hepatic fatty acid and cholesterol synthesis rates by reductions of several lipogenic genes. Interestingly, two groups demonstrated evidence that the hepatitis C virus genome has predicted binding sites of miR-122 and that miR-122 positively regulated the replication hepatitis C virus in human liver (Jopling et al. 2005, Randall et al. 2007). In addition to miR-122a, we found that miR-101b expression was upregulated in mouse liver development. Furthermore, upregulation of miR-101b and miR-122a expression was observed in the *in vitro* cultured of fetal hepatocytes treated with OsM and Dex (see Supplementary Figure 4A–C in the online version of this article). It has been reported that miR-101 is related to the immune system and megakaryocytopoiesis (Yu D et al. 2007, Garzon et al. 2006); however, the role of miR-101 in the liver has not yet been examined.

During early development in mice, haematopoietic stem cells emerge in the aorta/gonado/mesonephros region and then the stem cells migrate and expand in the fetal liver before haematopoiesis takes place in the bone marrow by the time of birth. Although most of the miRNAs that we observe in the liver developmental process are constitutively expressed, specific miRNAs are enriched at distinct stages of haematopoietic development. We found that the expression of miR-142-5p, miR-223 and miR-451 was downregulated in the process of liver maturation. As it has been reported that miR-142-5p and miR-142-3p are highly expressed in all haematopoietic tissues (Chen et al. 2004), miR-142 may thus play a critical role at the early stage of haematopoiesis. The expression of miR-223 was mainly detected in bone marrow and negatively regulated myeloid progenitor proliferation and granulocytic differentiation and activation (Johnnidis et al. 2008). In addition, miR-451 expression was upregulated during erythroid differentiation, and gain- and loss-of-function studies disclosed that miR-451 was related to erythroid maturation (Zhan et al. 2007).

Recent studies have indicated that a decrease of mature miRNA expression by impaired miRNA processing accelerates tumorigenesis and that a global reduction of miRNAs is observed in human cancers, suggesting that the role of overall miRNAs is to guard against oncogenic transformation (Kumar et al. 2007, Lu et al. 2005). In particular, the let-7 family is broadly known as a tumour suppressor. It has been reported that a decrease of let-7 expression was observed in human lung cancer and that let-7 negatively regulates the expression of H-ras and *HMGA2* oncogenes in breast cancer cells (Johnson et al. 2005, Yu F et al. 2007, Takamizawa et al. 2004). In addition, miR-16 was also reported as a tumour suppressor by inducing apoptosis mediated by Bcl-2 and modulating the cell cycle (Cimmino et al. 2005, Linsley et al. 2007). In a study of liver carcinogenesis, a decrease of miR-122 expression was observed in rat liver tumour (Kutay et al. 2006). Consistent with this report, miR-122a and miR-101b expression levels in 40 pairs of malignant neoplasias of hepatocyte lineage and adjacent non-tumorous tissue were reduced significantly ($p<0.05$, $n=40$) in tumour samples (see Supplementary Figure 4D in the online version of this article). However, in previous studies, it has been revealed that specific miRNAs acted as oncogenes, as their overexpression facilitates cancer progression. For example, miR-17-92 polycistron was overexpressed in lymphomas, lung cancers and colorectal cancers and enhanced cell proliferation (He et al. 2005, Hayashita et al. 2005). Furthermore, the copy number and expression level of miR-155 and its non-coding RNA transcript BIC were greatly increased in B-cell lymphomas (Eis et al. 2005). Our data show that the expression profile of oncogenic miRNAs was downregulated and, vice versa, the expression of tumour-suppressor miRNAs was upregulated in the process of liver development (Figure 4). This suggests that elevated oncogenic miRNAs are important

at the early developmental stage of the liver because, in this period, cell proliferation is frequent; in contrast, upregulation of tumour suppressor miRNAs is essential for preventing abnormal cell proliferation at the late stage of liver development. Therefore, our data suggest that the tight regulation of expression of cancer-related miRNAs (both oncogenic miRNAs and tumour suppressor miRNAs) occurred during normal liver development.

Finally, we have documented dynamic changes in miRNA expression that were found in the process of mouse liver development and some of them behaved as an oncofetal miRNA in HCC. Although little is known about the expression regulations, targets or roles of miRNAs in the liver, the expression profiles of miRNA in development could be informative with respect to the elucidation of the process of the development and diagnosis of cancer because the expression of some of the cancer-related miRNAs dramatically changed. Further studies on the differential expression of miRNA in liver development could contribute to a better understanding of the process of liver development and embryonic haematopoiesis and could facilitate the discovery of candidate miRNAs for cancer diagnosis and therapeutic targets in liver cancer.

Acknowledgements

We thank Dr Lim Chun Ren and Dr Kenichi Matsubara at DNA Chip Research Inc. for supporting the processing of microarray data. We thank Ms Ayako Inoue and Ms Nachi Namatame for their excellent technical assistance. This work was supported in part by a Grant-in-Aid for the Third-Term Comprehensive 10-Year Strategy for Cancer Control; Health Science Research Grants for Research on the Hepatitis C Virus from the Ministry of Health, Labour, Welfare of Japan; the Program for Promotion of Fundamental Studies in Health Sciences of the National Institute of Biomedical Innovation (NiBio); a Grant for Research Fellowships of the Japan Society for the Promotion of Science for Young Scientists.

Declaration of interest: The authors report no conflicts of interest. The authors alone are responsible for the content and writing of this article.

References

Ambros V. (2004). The functions of animal microRNAs. Nature 431:350-5.

Bartel DP. (2004). MicroRNAs: genomics, biogenesis, mechanism, and function. Cell 116:281-97.

Chen CZ, Li L, Lodish HF, et al. (2004). MicroRNAs modulate hematopoietic lineage differentiation. Science 303:83-6.

Chen JF, Mandel EM, Thomson JM, et al. (2006). The role of microRNA-1 and microRNA-133 in skeletal muscle proliferation and differentiation. Nat Genet 38:228-33.

Chim SS, Shing TK, Hung EC, et al. (2008). Detection and characterization of placental microRNAs in maternal plasma. Clin Chem 54:482-90.

Cimmino A, Calin GA, Fabbri M, et al. (2005). miR-15 and miR-16 induce apoptosis by targeting BCL2. Proc Natl Acad Sci U S A 102:13944-9.

Eis PS, Tam W, Sun L, et al. (2005). Accumulation of miR-155 and BIC RNA in human B cell lymphomas. Proc Natl Acad Sci U S A 102:3627-32.

Esau C, Davis S, Murray SF, et al. (2006). miR-122 regulation of lipid metabolism revealed by *in vivo* antisense targeting. Cell Metab 3:87-98.

Esquela-Kerscher A, Slack FJ. (2006). Oncomirs - microRNAs with a role in cancer. Nat Rev Cancer 6:259-69.

Fu H, Tie Y, Xu C, et al. (2005). Identification of human fetal liver miRNAs by a novel method. FEBS Lett 579:3849-54.

Garzon R, Pichiorri F, Palumbo T, et al. (2006). MicroRNA fingerprints during human megakaryocytopoiesis. Proc Natl Acad Sci U S A 103:5078-83.

Gilad S, Meiri E, Yogev Y, et al. (2008). Serum microRNAs are promising novel biomarkers. PLoS ONE 3:e3148.

Gramantieri L, Ferracin M, Fornari F, et al. (2007). Cyclin G1 is a target of miR-122a, a microRNA frequently down-regulated in human hepatocellular carcinoma. Cancer Res 67:6092-9.

Han J, Lee Y, Yeom KH, et al. (2006). Molecular basis for the recognition of primary microRNAs by the Drosha-DGCR8 complex. Cell 125:887-901.

Hayashita Y, Osada H, Tatematsu Y, et al. (2005). A polycistronic microRNA cluster, miR-17-92, is overexpressed in human lung cancers and enhances cell proliferation. Cancer Res 65:9628-32.

He L, He X, Lim LP, et al. (2007). A microRNA component of the p53 tumour suppressor network. Nature 447:1130-4.

He L, Thomson JM, Hemann MT, et al. (2005). A microRNA polycistron as a potential human oncogene. Nature 435:828-33.

Johnnidis JB, Harris MH, Wheeler RT, et al. (2008). Regulation of progenitor cell proliferation and granulocyte function by microRNA-223. Nature 451:1125-9.

Johnson SM, Grosshans H, Shingara J, et al. (2005). RAS is regulated by the let-7 microRNA family. Cell 120:635-47.

Jopling CL, Yi M, Lancaster AM, et al. (2005). Modulation of hepatitis C virus RNA abundance by a liver-specific MicroRNA. Science 309:1577-81.

Ketting RF, Fischer SE, Bernstein E, et al. (2001). Dicer functions in RNA interference and in synthesis of small RNA involved in developmental timing in *C. elegans*. Genes Dev 15:2654-9.

Kumar MS, Lu J, Mercer KL, et al. (2007). Impaired microRNA processing enhances cellular transformation and tumorigenesis. Nat Genet 39:673-7.

Kutay H, Bai S, Datta J, et al. (2006). Downregulation of miR-122 in the rodent and human hepatocellular carcinomas. J Cell Biochem 99:671-8.

Lawrie CH, Gal S, Dunlop HM, et al. (2008). Detection of elevated levels of tumour-associated microRNAs in serum of patients with diffuse large B-cell lymphoma. Br J Haematol 141:672-5.

Lee Y, Kim M, Han J, et al. (2004). MicroRNA genes are transcribed by RNA polymerase II. Embo J 23:4051-60.

Linsley PS, Schelter J, Burchard J, et al. (2007). Transcripts targeted by the microRNA-16 family cooperatively regulate cell cycle progression. Mol Cell Biol 27:2240-52.

Li QJ, Chau J, Ebert PJ, et al. (2007). miR-181a is an intrinsic modulator of T cell sensitivity and selection. Cell 129:147-61.

Lu J, Getz G, Miska EA, et al. (2005). MicroRNA expression profiles classify human cancers. Nature 435:834-8.

Lund E, Guttinger S, Calado A, et al. (2004). Nuclear export of microRNA precursors. Science 303:95-8.

Mitchell PS, Parkin RK, Kroh EM, et al. (2008). Circulating microRNAs as stable blood-based markers for cancer detection. Proc Natl Acad Sci U S A 105:10513-18.

Nelson PT, Hatzigeorgiou AG, Mourelatos Z. (2004). miRNP:mRNA association in polyribosomes in a human neuronal cell line. RNA 10:387-94.

Randall G, Panis M, Cooper JD, et al. (2007). Cellular cofactors affecting hepatitis C virus infection and replication. Proc Natl Acad Sci U S A 104:12884–9.

Shan Y, Zheng J, Lambrecht RW, et al. (2007). Reciprocal effects of micro-RNA-122 on expression of heme oxygenase-1 and hepatitis C virus genes in human hepatocytes. Gastroenterology 133:1166–74.

Takamizawa J, Konishi H, Yanagisawa K, et al. (2004). Reduced expression of the let-7 microRNAs in human lung cancers in association with shortened postoperative survival. Cancer Res 64:3753–6.

Yu D, Tan AH, Hu X, et al. (2007). Roquin represses autoimmunity by limiting inducible T-cell co-stimulator messenger RNA. Nature 450:299–303.

Yu F, Yao H, Zhu P, et al. (2007). Let-7 regulates self renewal and tumorigenicity of breast cancer cells. Cell 131:1109–23.

Zhan M, Miller CP, Papayannopoulou T, et al. (2007). MicroRNA expression dynamics during murine and human erythroid differentiation. Exp Hematol 35:1015–25.

Zhao Y, Ransom JF, Li A, et al. (2007). Dysregulation of cardiogenesis, cardiac conduction, and cell cycle in mice lacking miRNA-1-2. Cell 129:303–17.

Synergistic interactions between the synthetic retinoid tamibarotene and glucocorticoids in human myeloma cells

Tomoya Fukui,[1,2] Yasuo Kodera,[1] Kazuto Nishio,[3] Noriyuki Masuda,[2] Tomohide Tamura[4] and Fumiaki Koizumi[1,5]

[1]Shien-Lab and Support Facility of Project Ward, and [4]Division of Internal Medicine, National Cancer Center Hospital, 5-1-1 Tsukiji, Tokyo 104-0045; [2]Department of Respiratory Medicine, Kitasato University School of Medicine, 1-15-1 Kitasato, Kanagawa 228-8555; and [3]Department of Genome Biology, Kinki University School of Medicine, 377-2 Ohno-Higashi, Osaka, Japan

(Received November 6, 2008/Revised February 25, 2009/Accepted March 2, 2009/Online publication April 16, 2009)

Tamibarotene (TM411) is a synthetic retinoic acid receptor-α/-β selective retinoid that is chemically more stable than all-*trans* retinoic acid. This study was designed to evaluate the activity of TM411 in multiple myeloma (MM) and the effects of TM411 combined with a glucocorticoid (GC). *In vitro*, five human myeloma cells were treated with TM411 alone, GC alone, or TM411 + GC. Cell survival was analyzed by the tetrazolium dye assay and the Hoechst 33342/propidium iodide double-staining method. The effect of TM411 + GC was assessed by the isobologram method. *In vivo*, the growth-inhibitory effects of the drugs on RPMI-8226 cell xenografts established in SCID mice were examined. The effects of the agents on IL-6-mediated signaling pathways were also analyzed by Western blotting. TM411 was 2- to 10-fold more potent, in terms of its growth-inhibitory effect, than all-*trans* retinoic acid. The combination of TM411 and GC was found to show a markedly synergistic interaction. While increased expressions of the IL-6 receptor, phosphorylated MAPK, and Akt were observed after exposure to GC, TM411 attenuated this increase in the expressions, suggesting that such modification of the effect of GC by TM411 might be the possible mechanism underlying the synergistic interaction. Furthermore, TM411 + GC showed a supra-additive inhibitory effect in a xenograft model as compared with TM411 or GC alone. These results imply that the combination of TM411 + GC might be highly effective against MM, and suggest the need for clinical evaluation of TM411 + GC for the treatment of MM. (*Cancer Sci* 2009; 100: 1137–1143)

Multiple myeloma (MM) remains an incurable malignant tumor of the plasma cells of the bone marrow, and the five-year survival rate has been estimated to be 15–20%.[1] Although high-dose chemotherapy with hematopoietic stem-cell support has been shown to extend the event-free and overall survival,[2–4] this aggressive approach is generally not suitable for elderly patients over the age of 65 years, even though they account for more than 60% of all newly diagnosed cases of MM. In this group of patients, conventional chemotherapy with alkylating agents and anthracyclines, and also glucocorticoids (GCs),[5,6] has remained the treatment of choice. New treatments are urgently needed in these patients, and recently, preclinical and clinical trials have shown that novel targeted therapies, including the use of retinoid,[7–9] offer great promise for an improved outcome in patients with MM.[10,11]

Tamibarotene (TM411, retinobenzoic acid) is a synthetic retinoic acid receptor (RAR)-α/-β-selective retinoid, does not bind to RAR-γ, and is chemically more stable than all-*trans* retinoic acid (ATRA) against light, heat, and oxidation (Fig. 1a).[12] Therefore, TM411 might be expected to have fewer adverse events related to stimulation of RAR-γ. It was reported that the adverse events associated with TM411 were generally milder compared with those associated with ATRA therapy in patients with acute promyelocytic leukemia (APL).[13] ATRA has previously been shown to inhibit the growth of human myeloma cells.[14–16] TM411 has also been shown to have antimyeloma activity,[8] and preclinical and early clinical trials of the drug are underway.

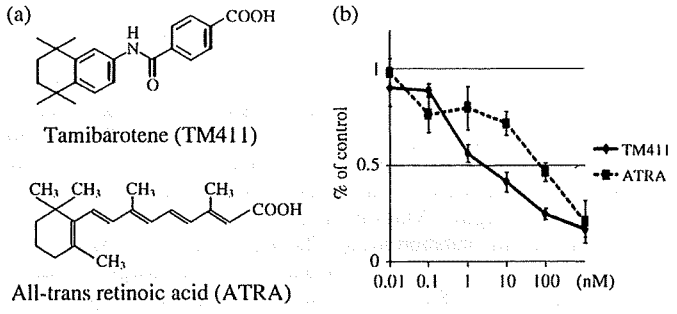

Fig. 1. (a) Structural formula of the two retinoids, tamibarotene (TM411) and all-*trans* retinoic acid (ATRA). (b) Growth-inhibitory effect of TM411 and ATRA on RPMI-8226 cells, determined by MTT assay. The cells were cultured with TM411 or ATRA (0.01–1000 nM) for 96 h. The growth-inhibition curves are shown. Points, mean values of at least three independent cultures; bars, SD.

The proliferation of MM cells triggered by cytokines such as IL-6, insulin-like growth factor-1, vascular endothelial growth factor, tumor necrosis factor-α, stromal cell-derived factor-1α, and IL-21 is mediated primarily through the MAPK signaling cascade. The cytokine-induced survival or resistance to apoptosis in myeloma cells is mediated through the JAK/STAT3 or PI3K/Akt pathways.[10] In these signaling cascades, IL-6-mediated signaling pathways are presumed to play a major role in the pathogenesis and malignant growth of MM by exerting an anti-apoptotic effect.[17–20] TM411, similar to ATRA, has been shown to inhibit IL-6 signaling.[21–23]

GCs such as dexamethasone (DEX) and prednisolone (PSL) are involved in the regulation of a variety of biological processes, including immune responses, metabolism, cell growth and proliferation, development, and reproduction. GCs induce apoptosis and have become key chemotherapeutic agents of many hematological malignancies including MM.[24,25] Although these drugs are frequently used to treat MM and are believed to induce apoptosis and cell cycle arrest of the tumor cells,[26] the precise mechanism of action has not yet been clearly elucidated.

[5]To whom correspondence should be addressed. E-mail: fkoizumi@ncc.go.jp

doi: 10.1111/j.1349-7006.2009.01155.x

Further, it was reported that GC not only triggered death signaling, but also simultaneously activated the IL-6 signaling pathway, which protects cells against DEX-induced apoptosis.[25]

In the present study, we evaluated the antitumor effect of the synthetic retinoid TM411 against human myeloma cells, and the combined effects of TM411 + GC, both *in vitro* and *in vivo*. In addition, we elucidated the biochemical mechanism underlying the synergistic interaction between the two agents through modulation of expression of the IL-6 receptor.

Materials and Methods

Agents. Tamibarotene (TM411, retinobenzoic acid) was provided by TMRC Co. Ltd (Tokyo, Japan). ATRA, DEX, and PSL were obtained from Sigma-Aldrich Japan (Tokyo, Japan). The drugs were dissolved in DMSO for the *in vitro* experiments, and TM411 and DEX were dissolved in ethanol and suspended in a 100-fold volume of PBS for the *in vivo* experiments.

Cells and culture. The human myeloma cell lines RPMI-8226 and U266 (American Type Culture Collection, Rockville, MD, USA), and MM.1S (Northwestern University, Chicago, IL,USA), and KMS-11 and KMS-12BM (Kawasaki Medical School, Okayama, Japan) were maintained in RPMI-1640 (Sigma-Aldrich Japan) supplemented with 10% heat-inactivated FBS (Life Technologies, Grand Island, NY, USA), and penicillin–streptomycin (Sigma-Aldrich Japan).

***In vitro* growth inhibition assay.** The tetrazolium dye (MTT) assay was used to evaluate the cytotoxicity of the drugs at various concentrations. A 180-μL volume of an exponentially growing cell suspension (1 to 2×10^4 cells/mL) was seeded into each well of a 96-well microculture plate containing 10% FBS medium and incubated for 24 h. The cells were exposed to 20 μL of each drug at various concentrations and cultured at 37°C in a humidified atmosphere for 96 h. After the culture period, 20 μL MTT solution (5 mg/mL in PBS) was added to each well and the plates were incubated for a further 4 h at 37°C. After centrifuging the plates at 200 *g* for 5 min, the medium was aspirated from each well, and 200 μL DMSO was added to each well to dissolve the formazan. The growth-inhibitory effect of each drug was assessed spectrophotometrically (SpectraMax 190; Molecular Devices, Sunnyvale, CA, USA).

Assessment of effect of TM411 + GC combination *in vitro*. The effects of TM411 + GC at the IC_{50} point were analyzed by the isobologram method[27] to evaluate the occurrence of synergism, additivity, or antagonism. For two drugs (A and B) that do not interact, the equation is: $(D)_A/(D_x)_A + (D)_B/(D_x)_B = 1$. In practice, the concentrations $(D_x)_A$, $(D_x)_B$, and $(D_x)_{A,B}$ for each of the drugs alone and the two drugs combined, respectively, required to produce the same percentage growth inhibition, are obtained from their dose–response curves. The concentrations of drugs A and B are plotted on the X and Y coordinates of the isobologram, respectively. Isoeffect curves are drawn, and the total area enclosed by the lines is considered to represent the 'envelope of additivity'. When the experimentally determined IC_{50} of the combination falls to the left side of the envelope, the interaction between the drugs used in combination is considered to be supra-additive (synergistic). When the experimental data point falls within the envelope, the combination is considered to exert an additive effect, and when it falls to the right side of the envelope but within the square produced by 0–1 IC_{50} units, the combination is considered to have sub-additive effects. When the point lies outside the square, the two drugs are considered to exert a protective effect against each other.

Western blot analysis. Cells were cultured overnight in 10% serum-containing medium. The cultured cells were washed twice with ice-cold PBS and lysed with M-PER Mammalian Protein Extraction Reagent (Pierce Biotechnology, Rockford, IL, USA) containing complete Mini (Roche Diagnostics, Mannheim, Germany) and Phosphatase Inhibitor Cocktail 1/2 (Sigma-Aldrich Japan). The protein concentration of the supernatants was determined by the BCA protein assay (Pierce Biotechnology). For preparation of the nuclear protein, the CelLytic NuCLEAR Extraction Kit (Sigma-Aldrich Japan) was used in accordance with the manufacturer's protocol. Then 20 μg samples of the cell lysates protein were electrophoretically separated on a Multigel II Mini (Daiichi Pure Chemicals, Tokyo, Japan) and transferred to a PVDF membrane (Millipore, Bedford, MA, USA). The membrane was incubated with antibodies against IL-6Rα, gp130, RAR-α, RAR-β, RAR-γ (Santa Cruz Biotechnology, Santa Cruz, CA, USA), Akt, phospho-Akt (Ser473), phospho-p44/42 MAPK (Thr202/204), phospho-MEK1/2 (Ser217/221), phospho-Stat3 (Tyr705), BAX, Bcl-xL, Mcl-1 (Cell Signaling Technology, Beverly, MA, USA), and β-actin (Sigma-Aldrich Japan) as the first antibody, followed by detection using an HRP-conjugated secondary antibody. The bands were visualized with an ECL detection reagent (Amersham, Piscataway, NJ, USA).

Cell survival assay. Cell viability was assessed morphologically by staining the nuclei of the cells with Hoechst 33342 and propidium iodide (PI), as previously described.[28] Hoechst 33342 and PI were purchased from Molecular Probes (Eugene, OR, USA). After incubation, the cells were collected and stained with Hoechst 33342 and PI for 15 min, then examined by fluorescence microscopy. The cell death induction ratio was calculated as the ratio of the number of cells containing PI-stained nuclei to the total number of cells (approximately 300–500 cells).

IL-6 ELISA. RPMI-8226 cells were rinsed twice in PBS (pH 7.4) and transferred to fresh culture medium at 1×10^4 cells/mL under serum-starvation conditions, and equal amounts of the cells were dispensed into three individual dishes. Following incubation for 48 h, aliquots of the medium were analyzed in triplicate using the human IL-6 ELISA (Bender Medsystems, Burlingame, CA, USA) to determine the levels of IL-6 secretion in accordance with the manufacturer's protocol.

Xenograft murine model. Four-week-old female mice with SCID were purchased from Charles River (Yokohama, Japan). All mice were maintained in a specific pathogen-free area in our animal resources facility. Five mice per group were given an s.c. injection into the right flank of 3×10^7 RPMI-8226 myeloma cells in 100 μL PBS, together with 100 μL Matrigel (BD Biosciences, Bedford, MA, USA). Tumor growth was monitored daily, and the mice were randomized to drug-treated or control groups when the tumor volume reached approximately 200 mm^3. Tumor-bearing mice were treated with either TM411 (2 mg/kg/day) by i.p. injection daily for 21 consecutive days, DEX (1 mg/kg/day) by i.p. injection on day 0–3, day 7–10, and day14–17, or both agents. In the control group, vehicle alone (PBS 100 μL/day) was injected i.p. by the same schedule as that of TM411. Tumor diameters were measured with calipers three times per week to evaluate the effects of the treatment, and the tumor volume was calculated by the following formula: $a \times b^2/2$ (mm^3), where a is the largest diameter of the tumor and b is the shortest diameter. All mice were killed when their tumors reached more than 2 cm in diameter or when the mice became moribund. Survival was evaluated from the first day of treatment until death. The protocol of the experiment was approved by the Committee for Ethics in Animal Experimentation, and conducted in accordance with the Guidelines for Animal Experiments of the National Cancer Center.

Statistical analysis. The statistical significance of differences among the experimental groups was determined using Student's *t*-test. The level of significance was set at $P < 0.05$. Overall survival in each treatment group was compared using Kaplan–Meier curves and log–rank tests. All analyses were carried out using the SPSS statistical software package (SPSS version 16.0 for Windows; SPSS, Chicago, IL, USA).

doi: 10.1111/j.1349-7006.2009.01155.x

Results

TM411 inhibited proliferation of human myeloma cell lines. We examined the growth-inhibitory effect of TM411 in the RPMI-8226, MM.1S, U266, KMS-11, and KMS-12BM cell lines by MTT assay. The IC_{50} value of TM411 was approximately 3 nM for RPMI-8226 and 10 nM for MM.1S cells. Thus, the growth-inhibitory effect of TM411 on the two cell lines was 2- to 10-fold more potent than that of ATRA (Fig. 1b). RPMI-8226 and MM.1S cells were also sensitive to GCs, including PSL and DEX, whereas the U266 and KMS-12BM cells were resistant to these agents, and the KMS-11 cells were resistant to TM411 (Table 1).

Expression levels of RARs observed in myeloma cells. We examined the expressions of the RARs by Western blot analysis of 20 μg nuclear extracts obtained from the myeloma cells. Comparison of the protein expression levels of RAR-α and RAR-β, which represented specific targets of TM411, in the myeloma cells revealed high expression levels of the receptors in the sensitive RPMI-8226 and MM.1S cells. The expressions were more subtle in the resistant U266 cells, and the resistant KMS-11 and KMS-12BM cells showed high expression levels of RAR-α and RAR-β. RAR-γ protein was detected in all five cell lines. (Fig. 2)

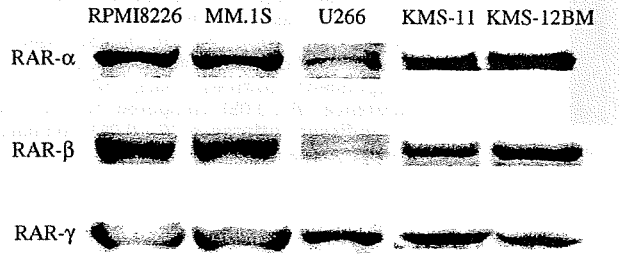

Fig. 2. Expression of retinoic acid receptors (RARs) in the three myeloma cell lines, RPMI-8226, MM.1S, U266, KMS-11, and KMS-12BM, determined by Western blot analysis. The nuclear protein was extracted from the myeloma cells and a 20 μg sample of the lysates was subjected to the analysis. The tamibarotene (TM411)-sensitive RPMI-8226 and MM.1S cell lines were found to overexpress RAR-α/-β, which are target receptors for TM411.

Marked synergistic interaction between TM411 and GCs observed *in vitro*. Based on the results of the evaluation of growth inhibition *in vitro* by the MTT assay, the effect of the combination of TM411 + GC was evaluated against the RPMI-8226 and MM.1S cells *in vitro*. The cells were cultured with TM411 for 96 h at various concentrations of TM411, in the presence or absence of GC. The growth rates were expressed as the averages of at least three independent experiments. The effect of combined of TM411 + DEX treatment on the RPMI-8226 cells is shown in Figure 3. MTT assay revealed that TM411 inhibited RPMI-8226 cell growth in a dose-dependent manner; moreover, the drug also synergistically enhanced the growth-inhibitory effect of DEX (Fig. 3a). The effects of combined TM411 + DEX treatment were further assessed by the *in vitro* isobologram method. The experimentally determined IC_{50} values of the combination fell to the left side of the envelope, therefore, the interaction between TM411 and DEX used in combination was considered to be synergistic (Fig. 3b).

Cell death increased by combined TM411 + GC treatment. To detect apoptosis and necrosis morphologically, Hoechst 33342 and PI nuclear staining was used. Cells were treated with either 6 nM TM411 (concentration twofold the IC_{50}), 100 nM PSL (concentration twofold the IC_{50}), 3 nM TM411 (IC_{50}) combined with 50 nM PSL (IC_{50}), or vehicle control for 24, 48, or 72 h. Then we randomly selected three visual fields for microscopy, and counted the total number of cells, and the number of apoptotic or necrotic cells. The cell death rate was determined as the average from three independent experiments. The cell death induction ratio was significantly higher in cultures treated with the combination of TM411 + PSL than in the cultures treated with TM411 or PSL alone (Fig. 4).

TM411 inhibited myeloma cell growth associated with downregulation of IL-6-related molecules. Because previous studies have shown that IL-6 is a major growth factor for myeloma cells both *in vitro* and *in vivo*,[29–32] we examined the modulation of IL-6-related molecules by combined TM411 + DEX treatment. We first examined the effect of TM411, DEX, and combined TM411 + DEX treatment on the level of IL-6 secretion from the RPMI-8226 cells using ELISA. The IL-6 secretion showed a trend towards decrease with the treatment, however, no significant differences were observed among the groups (Fig. 5a). We next examined the expression of IL-6 receptor-α and gp130 by

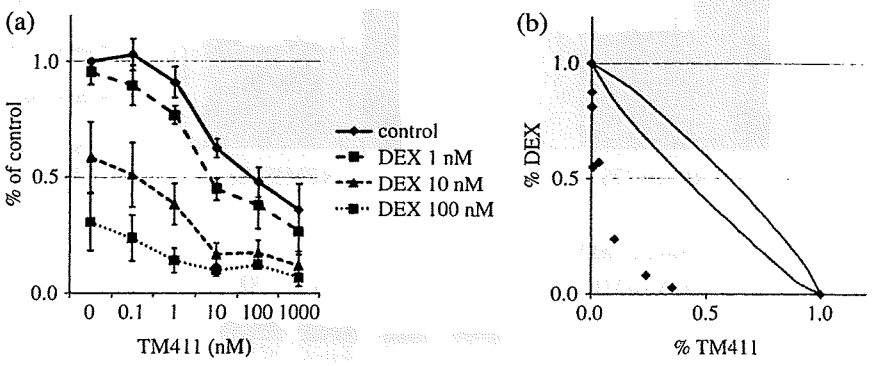

Fig. 3. Effects of combined tamibarotene (TM411) + dexamethasone (DEX) treatment on RPMI-8226 cells, determined by MTT assay. (a) The growth-inhibition curves for RPMI-8226 treated with TM411 with or without DEX are shown. Points, mean values of at least three independent cultures; bars, SD. (b) Isoborogram of the interactions between TM411 and DEX in RPMI-8226 cells. The effect of combined TM411 + DEX treatment was analyzed at the 50% growth inhibition ratio points. The experimentally determined IC_{50} values of the combination fell to the left side of the envelope, and the drugs were judged to exert synergistic effects.

Table 1. ***In vitro*** **growth-inhibitory effects in human myeloma cells by MTT assay**

IC_{50} (μM)	RPMI-8226	MM.1S	U266	KMS-11	KMS-12BM
TM411	0.0031 ± 0.0018	0.0095 ± 0.0110	37.80 ± 13.80	44.800 ± 26.100	12.2 ± 7.0
ATRA	0.0780 ± 0.0260	0.4200 ± 0.5000	14.00 ± 8.40	N.D.	N.D.
DEX	0.0280 ± 0.0340	0.0190 ± 0.0013	66.36 ± 18.10	0.037 ± 0.023	>100
PSL	0.1100 ± 0.0680	0.0710 ± 0.0190	>100	N.D.	N.D.

Each value is the mean ± SD. ATRA, all-*trans* retinoic acid; DEX, dexamethasone; N.D., not done; PSL, prednisolone; TM411, tamibarotene.

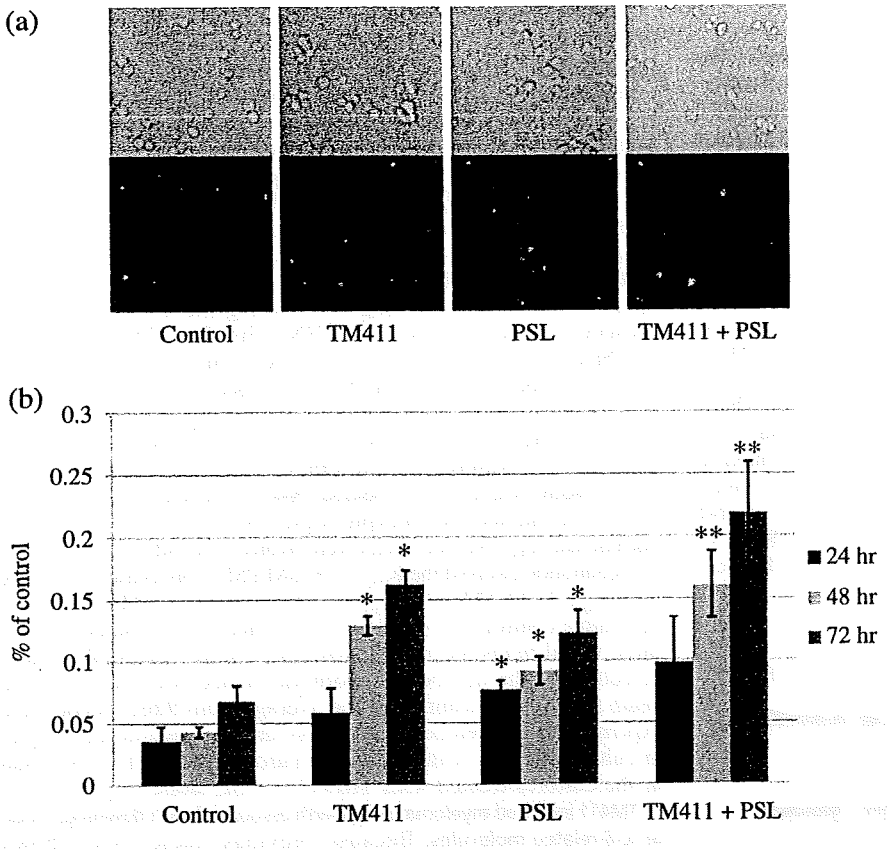

Fig. 4. The cytotoxixcity of tamibarotene (TM411) in the presence or absence of prednisolone (PSL) was evaluated morphologically by the Hoechst 33342/propidium iodide double-staining method. RPMI-8226 cells were cultured in either control medium, or medium containing TM411 (6 nM; concentration twofold the IC_{50}), PSL (100 nM; concentration twofold the IC_{50}), or TM411 (3 nM; IC_{50}) in combination with PSL (50 nM; IC_{50}) for 24, 48 or 72 h. At the end of the incubation period, the cells were stained with Hoechst 33342 (blue) and propidium iodide (red) for 15 min and examined under a fluorescence microscope. (a) Fragmented cells stained blue or red with condensed nuclei correspond to apoptotic cells, whereas cells stained blue with round nuclei correspond to viable cells. (b) We counted the total number of cells and number of apoptotic cells in each visual field, and calculated the cell death induction ratio as the ratio of the number of apoptotic cells to the total number of cells in three visual fields. The cell death induction ratio at 72 h was significantly higher in the TM411 + PSL group than in the PSL alone group ($P = 0.019$). Colums, mean values of three independent cultures; bars, SD. *Significant difference ($P < 0.05$) compared to the control; **significant difference ($P < 0.05$) compared to the PSL alone group.

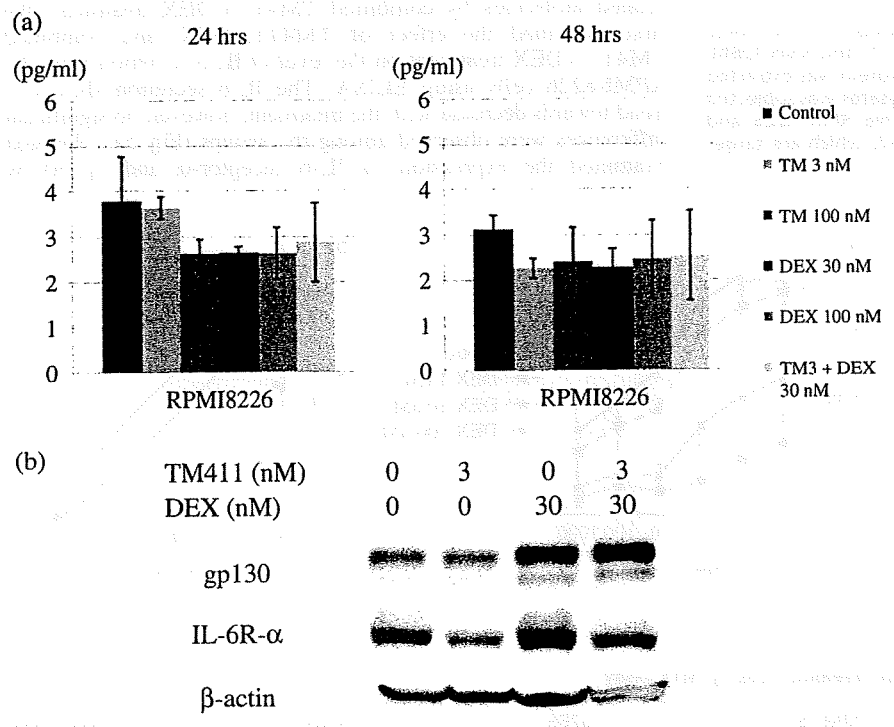

Fig. 5. Tamibarotene (TM411) modulates the expression of IL-6-related molecules. (a) Supernatant was collected from RPMI-8226 cells treated with TM411 (3 nM, IC_{50}; 100 nM, IC_{80}) in the presence or absence of dexamethasone (DEX) (30 nM, IC_{50}; 100 nM, IC_{80}) for 24 or 48 h. IL-6 was measured by ELISA ($n = 3$ experiments each). No significant change in the amount of IL-6 secreted was observed after exposure to the drugs. Columns, mean values of three independent cultures; bars, SD. (b) RPMI-8226 cells were treated with TM411 (3 nM) in the presence or absence of DEX (30 nM) for 24 h. A 20-μg sample of the cell lysates was subjected to Western blot analysis to assess the protein expressions of the IL-6 receptor (IL-6R)-α, gp130, and β-actin (control). Treatment with DEX increased the expressions of both IL-6R-α and gp130. TM411 inhibited the expression of IL-6R-α. The expression of IL-6R-α induced by DEX was also inhibited by TM411.

Western blotting. IL-6 receptor-α expression in the RPMI-8226 cells was downregulated by TM411. Although increased expression of IL-6 receptor-α was observed after exposure to DEX, TM411 inhibited this increase of expression induced by DEX. However, TM411 had no inhibitory effect on the increased expression of gp130 induced by DEX (Fig. 5b).

TM411 modulated IL-6-triggered signaling cascades. Given that TM411 inhibited the expression of IL-6 receptor-α, we examined

doi: 10.1111/j.1349-7006.2009.01155.x

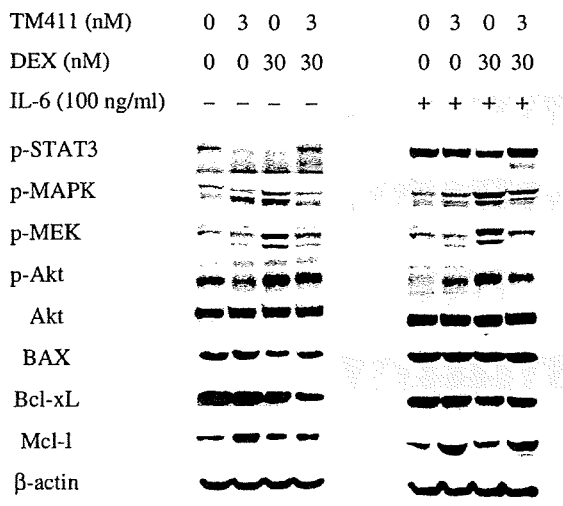

Fig. 6. Regulation of IL-6-mediated signaling cascades. (a) RPMI-8226 cells were pretreated with tamibarotene (TM411) (3 nM, IC_{50}) in the presence or absence of dexamethasone (DEX) (30 nM, IC_{50}) for 24 h. Samples (20 μg) of the cell lysates were subjected to Western blot analysis to assess the phosphorylation status and protein expression levels of STAT3, MAPK, MEK, Akt, BAX, Bcl-xL, Mcl-l and β-actin. The phosphorylations of MAPK and Akt induced by DEX were inhibited by TM411.

the effects on the IL-6-triggered signaling cascades. RPMI-8226 cells were cultured with TM411 for 24 h. We showed that treatment with DEX alone increased the expression of phosphorylated MAPK, MEK, and Akt, which might be protective signals against DEX-induced apoptosis,[25] in the RPMI-8226 cells stimulated or not stimulated with IL-6 (100 ng/mL). The increase in the expressions of phosphorylated MAPK and Akt induced by DEX was attenuated by combined treatment with TM411 (Fig. 6). The findings suggest that such modification by TM411 of the effects of DEX might be the possible mechanism underlying the synergistic effect of TM411 and GC.

TM411 inhibited human myeloma cell growth and enhanced cytotoxicity of GC *in vivo*. In order to confirm whether combined TM411 + GC treatment exerted a synergistic effect, the growth-inhibitory effect of the combination was evaluated *in vivo* using a xenograft murine model. The mice were given i.p. injections of either TM411 (2 mg/kg/day) on days 0–20, or DEX (1 mg/kg/day) on days 0–3, 7–10, and 14–17, both TM411 and DEX, or only vehicle control for 21 days (Fig. 7a), the first treatment day being defined as day 0. Treatment with TM411 or DEX alone suppressed the tumor growth compared with that in the control. Moreover, combined TM411 + DEX treatment induced more potent growth inhibition of the tumor (Fig. 7b,c). No significant body weight loss was observed in any of the groups (Fig. 7d). We also observed significantly prolonged survival in the animals treated with the combination than in the other groups (Fig. 7e). These results confirm the activity of TM411 as an antimyeloma agent with less toxicity and also the more marked growth-inhibitory effect of combined TM411 + DEX use against a tumor xenograft of MM.

Discussion

Retinoids have been indicated to have antitumor activity.[33] In particular, ATRA has been used successfully in patients with APL, and significant clinical responses have also been obtained in other malignancies. The growth-inhibitory effect of ATRA on MM cells has also been shown.[15,34,35] However, ATRA alone was found to be ineffective in pretreated MM patients with toxicity,[7] therefore, it was not developed for clinical use. Tamibarotene (TM411) is a synthetic RAR-α/-β selective retinoid[12] approved for use in the treatment of relapsed or refractory APL in Japan. Compared to ATRA, which is indicated for the first-line treatment of APL, TM411 is characterized by greater chemical stability, is a more potent inducer of differentiation in APL cells, and shows a lower potential for drug resistance.[12] Furthermore, the adverse events of this drug have also been shown to be milder than those of ATRA in clinical trials.[13] TM411 is being investigated in clinical trials for the treatment of MM, with the objective of confirming the greater therapeutic advantage of this drug as compared to ATRA.

In the present study, we illustrated the cytotoxic activity of TM411 against human myeloma cells. It is well known that IL-6 signaling plays an important role in the growth of MM, both *in vitro* and *in vivo*.[15,17,36–39] IL-6 acts as a potent survival and anti-apoptotic factor in MM through activation of multiple signaling cascades. Previous studies have shown that IL-6 induces growth and survival of human myeloma cells by way of the MAPK,[40] JAK/STAT,[31,41,42] and PI3K/Akt kinase pathways, which inhibit apoptosis and the appearance of drug resistance in MM cells.[32,43] Our data indicated that TM411 induced IL-6 receptor-α downregulation and inhibited its downstream signaling molecules, such as MAPK and Akt. These effects might be responsible for the observed growth-inhibitory effect of the drug on myeloma cells *in vitro* and *in vivo*. Similarly, the inhibitory effect of ATRA on the growth of MM cells was determined to be through the regulation of an IL-6 receptor-related signaling pathway.[15,44]

The *in vitro* and *in vivo* experiments in our study showed the synergistic potential of the combination of TM411 + GC. GCs such as DEX and PSL induce apoptosis through transcriptional activation of death-specific genes in hematological cells, including leukemia, lymphoma, and myeloma.[26] GC not only triggers death signaling, but also simultaneously activates a protective signal, whereby increased IL-6 receptor expression on the MM cell surface facilitates enhanced IL-6 binding and related protection against GC-induced apoptosis.[25] IL-6 not only triggers myeloma cell growth through the MAPK signaling cascade,[40] but also blocks DEX-induced apoptosis by activation of the PI3K/Akt pathway,[32] therefore, our data suggested that the inhibitory effect of TM411 on GC-mediated anti-apoptotic signaling molecules might represent synergistic interaction.

Increased phosphorylation of MAPK, MEK, and Akt was observed in RPMI-8226 cells exposed to GC. Activation of the MAPK and Akt pathways by GCs might elicit a survival response against apoptosis[30,32,45,46] and such activation was inhibited partially by TM411. Increase in the expression of phosphorylated STAT3 was observed only when the cells were exposed to TM411 in combination with a GC. Although STAT3 is one of the key molecules that promote cell growth in MM, the reason for this modification occurring only in the combination setting is unclear. We examined the expression of the downstream molecules of STAT3 such as pro-apoptotic protein BAX, anti-apoptotic protein Bcl-xL and Mcl-1 by Western blot analysis. As a result, we observed that the expression of Bcl-xL was decreased in the combination of TM411 + DEX compared with the treatment of TM411 or DEX alone, and those of Mcl-1 was decreased in the combination compared with the treatment of TM411 alone without IL-6 stimulation. We suggested the treatment of TM411 combined with DEX might promote apoptosis compared with DEX alone, but could not show the significant modulations of STAT3-related molecules by these drugs, therefore further study is required.

In younger patients with MM, high-dose chemotherapy with hematopoietic stem cell transplantation is a useful approach with survival benefit, but is generally not suitable for patients older than 65 years because of its severe toxicity. Recently,

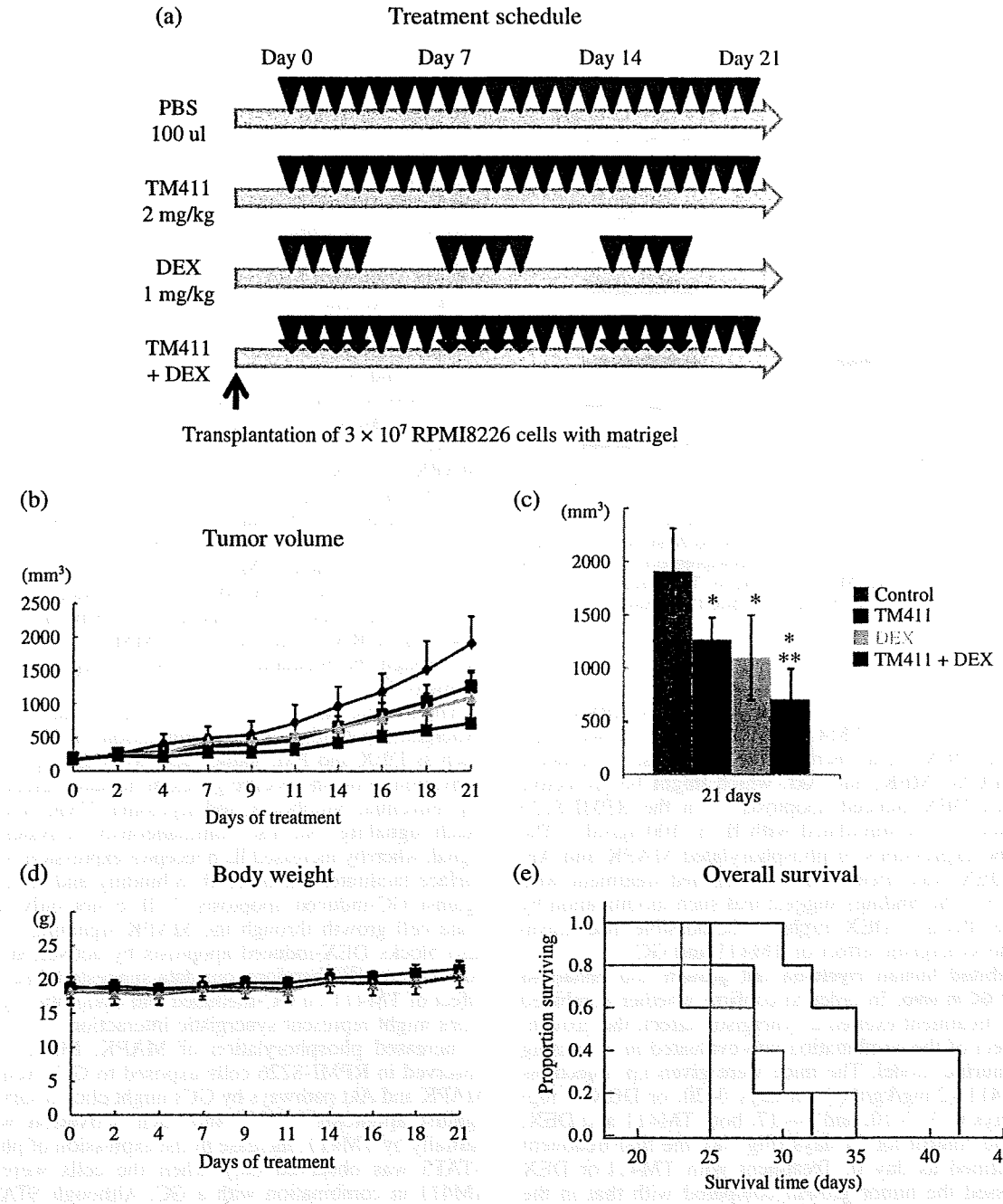

Fig. 7. Combined effects of tamibarotene (TM411) + dexamethasone (DEX) on RPMI-8226 tumor xenografts *in vivo*. (a) Treatment schedule. (b) Mice were randomized to four groups (five mice/group). The tumor volume was calculated as described in Materials and Methods. Each data point represents the mean tumor volume of the five mice in each group. Significant growth inhibition was observed in the mice treated with TM411 + DEX. (c) Histogram of the mean tumor volume and statistical analysis on day 21. Columns, mean values of five mice; bars, SD. *Significant difference ($P < 0.05$) compared to the control; **significant difference compared to the TM411 alone group ($P < 0.01$). (d) Body weight change was evaluated three times per week. Points, mean values of five mice in each treatment group; bars, SD. (e) Overall survival was evaluated from the first day (day 0) of treatment until death using Kaplan–Meier curves. The TM411- and DEX-treated mice showed longer overall survival than the control mice ($P = 0.012$ and 0.080, respectively); moreover, the mice treated with TM411 + DEX also showed longer survival than those treated with TM411 ($P = 0.017$) or DEX ($P = 0.048$) alone.

novel biologically-based treatments such as thalidomide,[47–50] lenalidomide,[51–53] and bortezomib[54,55] have been shown to exert marked activity against MM in clinical trials, but specific toxicity profiles, such as myelosuppression and neurotoxicity, remain clinical problems.[10] The present data suggest that TM411 given in combination with a GC is one of the most promising therapeutic regimens for MM, especially in high-risk patients, however, further studies are required to verify the feasibility of use of the combination in the clinical setting.

Acknowledgments

This study was supported in part by a Research Resident Fellowship from the Foundation for Promotion of Cancer Research (Japan) for the 3rd Term Comprehensive 10-Year Strategy for Cancer Control (T. Fukui). We thank Yuka Kitamura (Shien-Lab and Support Facility of Project Ward, National Cancer Center Hospital), Takashi Watanabe and Kumiko Nagase (Hematology and Stem Cell Transplantation Divisions, National Cancer Center Hospital) for their technical support.

doi: 10.1111/j.1349-7006.2009.01155.x